granuloma [15,16]. These models not only exhibit structural similarities to granulomas observed in human clinical specimens, but also show patterns of cell antigen expression and/or cytokine production that appear consistent with those observed in tuberculosis patients. However, the formation of granulomas in leprosy, involving *M. leprae* infection has not been previously studied in vitro. The only data available on granuloma formation of leprosy is from the immunological staining of biopsies of patients, and granulomas harvested from the footpads of athymic nude mice [27].

In our model, we first infected the immature human macrophages with *M. leprae*. To mimic the recruitment of additional PBMCs which would occur in vivo, autologous PBMCs were added after 24 h and cultured at 35° C, the optimal temperature for the growth of *M. leprae* and macrophages to be kept viable. Within 9 days of culture, macrophages and T lymphocytes gathered to form a granuloma-like aggregates with fused macrophages, appearing as multinucleated cells, and epitheloid macrophages tightly linked to surrounding macrophages and lymphocytes. However, in control groups, the formation of granuloma-like aggregates was not observed. When autologous T lymphocytes and monocytes were purified and used instead of PBMCs, a similar formation of granuloma like aggregates were observed, together with production of the same amounts of cytokines, indicating that T lymphocytes and monocytes are sufficient for the containment of *M. leprae* in granuloma like structures.

Electron microscopy studies indicated that the tuberculoid lesion had an appearance of a granulomatous response with a predominance of ECs and MGCs, and the mononuclear phagocytes which are surrounded by a mantle of lymphocytes [28]. In the present *in vitro* model of granulomas, MGCs were prominent, and resembled MGCs observed in a tuberculoid lesion. MGCs have been described by Langhans, but the function of these cells in the granuloma remains to be elucidated [29]. In this study, we observed not only Langhans giant cells (MGCs with a circular nuclear organization in contrast to the MGCs formed in response to a foreign body that lacks this kind of organization), but also the bacilli surrounded by nuclei and restricted to the central cytoplasmic region. Because this type of MGC is not observed in the normal mouse model, it is interesting to further focus on the formation, mechanism and function of such MGCs using human *in vitro* model or humanized mouse model as recently described by Heuts et al. [30]. The *in vitro* model of leprosy granulomas still needs to be investigated, and compared to that obtained using leprosy patients' monocytes and T cells.

Macrophages function as control switches of the immune system, providing a balance between pro- and anti-inflammatory responses by developing into subsets of M1 or M2 activated macrophages. M1 macrophages are activated by type I cytokines such as IFN-γ and TNFα, Alternatively, activated M2 macrophages are subdivided further into M2a (activated by IL-4 or IL-13), M2b (activated by immune complexes in combination with IL-1β) and M2c (activated by IL-10 or glucocorticoids) [31]. M1 macrophages exhibit a potent microbicidal activity, and release IL-12, promoting strong Th1 immune responses. It is the M1 population that is thought to contribute to macrophage-mediated tissue injury [19,32]. In contrast, M2 macrophages support Th2-associated effector functions and exert a selective immunosuppressive activity. M2 macrophages also play a role in the resolution of inflammation through phagocytosis of apoptotic neutrophils, reduced production of pro-inflammatory cytokines, and increased synthesis of mediators that are important for tissue remodeling and wound repair. We investigated the contribution of the macrophage polarization, MGC formation and immune responses against *M. leprae* in granulomas, and found that there was a strong relationship between the formation of granuloma-like aggregates, the changes of cell surface antigen expression on macrophages, and the expression levels of various cytokines with the macrophage polarization. In *M. leprae* infected macrophages co-cultured with PBMCs, the concentrations of IL-2, IL-12 and TNF-α peaked at day 1, while, TLR4, CD86, and MHC molecules were highly expressed, indicating that most of the macrophages were of the M1 subset. At day 9, in the same group of infected macrophages co-cultured with PBMCs, the cells assembled and formed a multilayer, granuloma-like aggregates, and the macrophages not only highly expressed TLR4 and CD86, but also scavenger receptor (CD163) and mannose receptor (CD206) molecules. CD163 and CD206 are the markers of M2 macrophages. Therefore, the M1 and M2 macrophages coexisted in granuloma-like aggregates. Consistent with this observation, the levels of IL-1β, IL-2, IL-12 and IFN-γ were high in the culture medium, promoting the differentiation of macrophages into both M1 and M2 subsets. The protective cell mediated immune response is regulated by the cytokine equilibrium, while the tuberculoid pole is characterized by the presence of Th1 cytokines (IL-2, IFN-γ, TNF-α and IL-12), and lepromatous is characterized by type 2 cytokines (IL-4, IL-6 and IL-10) [33]. Because IL-10 is an immunosuppressive cytokine implicated in susceptibility to mycobacterial infection, we examined the expression of IL-10 in more detail. Indeed, the infection with *M. leprae* suppressed the production of IL-10. However, when macrophages were differentiated with M-CSF, rather than GM-CSF, *M. leprae* infection further enhanced IL-10 production. Our results indicate that the granuloma aggregates studied here, are similar to those observed in the tuberculoid form of leprosy. However, little is known about the type

of cytokines that influence the formation of macrophages for containment of *M. leprae* in the granulomas during the pathogenesis of leprosy.

We also investigated the viability of *M. leprae* in macrophages at different time points. At day 9, a number of granuloma-like aggregates were observed in co-cultures of PBMCs with macrophages infected with *M. leprae*. However in macrophages infected with *M. leprae* without the PBMCs, granuloma-like aggregates were not observed. There were no significant differences in the viability of *M. leprae* in macrophage of different groups on day 1, but on day 9, the viability of *M. leprae* in the group that formed granuloma-like aggregates was slightly lower, although not significantly, than that of *M. leprae* in infected macrophages without PBMCs. Evidently, granuloma-like aggregates appear to benefit the host but the bacilli remained metabolically active. The mechanism of this phenomenon needs further in-depth analysis.

Conclusions

In summary, we have developed for the first time a method to obtain *in vitro M. leprae* granulomas using human monocyte derived macrophages and PBMCs. Using this model, we obtained some basic information about the characteristics of *in vitro* granulomas. In addition, the viability of *M. leprae* in granuloma-like aggregates remained unaltered during the culture period. Effective strategies to allow the bacilli to succumb to the formation of granuloma may assist in the primary control of the infection.

Additional file

Additional file 1: Figure S1. Measurement of IL-10 secreted into the culture medium by ELISA. Measurement of IL-10 secreted in the culture medium from different groups of cells at days 2, 6 and 9 is shown. Two types of macrophages were used to analyze the data. (A) Macrophages differentiated using GM-CSF, and (B) macrophages differentiated from monocytes using M-CSF. Representative data from two individual experiments of a single donor are shown. Unpaired student's t test was performed, *$p < 0.0001$, **$p < 0.001$, ***$p < 0.05$.

Abbreviations

DCs: Dendritic cells; PBMCs: Peripheral blood mononuclear cells; ECs: Epitheloid cells; MGCs: Multinucleated giant cells; BCG: Bacillus Calmette- Guérin.

Competing interests

The authors declare that they have no competing interests.

Authors' contributions

HW, YM participated in the design of the study and carried out the cell culture experiments, YF carried out the confocal microscopic examination, and radio-respirometric assay. HW, YM, and MM were involved in the preparation of the manuscript. All authors have read and approved the final manuscript.

Acknowledgments

This study was supported by grants from the Grant-in-Aid from the Ministry of Health, Labor and Welfare of Japan for "Research on Emerging and Re-emerging Infectious Diseases" (Grant no. H24-Shinko-Ippan-009 to YM) and also from the National Natural Science Foundation of China (30972651), the fund for Key Clinical Program of the Ministry of Health (2010-2012-125). We appreciate the helpful assistance of Drs. Masanori Matsuoka and Masanori Kai for the *M. leprae* propagation and isolation. We also thank the Japanese Red Cross Society for kindly providing whole blood cells from healthy donors.

Author details

[1]Institute of Dermatology, Chinese Academy of Medical Sciences and Peking Union Medical College, 12 Jiangwangmiao Road, Nanjing 210042, China. [2]Department of Mycobacteriology, Leprosy Research Center, National Institute of Infectious Diseases, 4-2-1 Aobacho, Higashimurayama, Tokyo 189-0002, Japan.

Received: 13 December 2012 Accepted: 17 June 2013
Published: 20 June 2013

References

1. Britton WJ: **Immunology of leprosy.** *Trans R Soc Trop Med Hyg* 1993, **87**:508–514.
2. Kaplan G, Cohn ZA: **The immunobiology of leprosy.** *Int Rev Exp Pathol* 1986, **28**:45–78.
3. Saunders BM, Cooper AM: **Restraining mycobacteria: role of granulomas in mycobacterial infections.** *Immunol Cell Biol* 2000, **78**:334–341.
4. Rojas-Espinosa O, Løvik M: ***Mycobacterium leprae* and *Mycobacterium lepraemurium* infections in domestic and wild animals.** *Rev Sci Tech* 2001, **20**:219–251.
5. Ulrichs T, Kaufmann SH: **New insights into the function of granulomas in human tuberculosis.** *J Pathol* 2006, **208**:261–269.
6. Clay H, Volkman HE, Ramakrishnan L: **Tumor necrosis factor signaling mediates resistance to mycobacteria by inhibiting bacterial growth and macrophage death.** *Immunity* 2008, **29**:283–294.
7. Dannenberg AM Jr: **Immunopathogenesis of pulmonary tuberculosis.** *Hosp Pract (Off Ed)* 1993, **28**(1):51–58.
8. Lesley R, Ramakrishnan L: **Insights into early mycobacterial pathogenesis from the zebrafish.** *Curr Opin Microbiol* 2008, **11**:277–283.
9. Tobin DM, Ramakrishnan L: **Comparative pathogenesis of *Mycobacterium marinum* and *Mycobacterium tuberculosis*.** *Cell Microbiol* 2008, **10**:1027–1039.
10. Davis JM, Ramakrishnan L: **The role of the granuloma in expansion and dissemination of early tuberculous infection.** *Cell* 2009, **136**:37–49.
11. Bouley DM, Ghori N, Mercer KL, Falkow S, Ramakrishnan L: **Dynamic nature of host-pathogen interactions in *Mycobacterium marinum* granulomas.** *Infect Immun* 2001, **69**:7820–7831.
12. Saunders BM, Frank AA, Orme IM, Cooper AM: **CD4 is required for the development of a protective granulomatous response to pulmonary tuberculosis.** *Cell Immunol* 2002, **216**:65–72.
13. Poey C, Verhaegen F, Giron J, Lavayssiere J, Fajadet P, Duparc B: **High resolution chest CT in tuberculosis: evolutive patterns and signs of activity.** *J Comput Assist Tomogr* 1997, **21**:601–607.
14. Tsai MC, Chakravarty S, Zhu G, Xu J, Tanaka K, Koch C, Tufariello J, Flynn J, Chan J: **Characterization of the tuberculous granuloma in murine and human lungs: cellular composition and relative tissue oxygen tension.** *Cell Microbiol* 2006, **8**:218–232.
15. Puissegur MP, Botanch C, Duteyrat JL, Delsol G, Caratero C, Altare F: **An in vitro dual model of mycobacterial granulomas to investigate the molecular interactions between mycobacteria and human host cells.** *Cell Microbiol* 2004, **6**:423–433.
16. Birkness KA, Guarner J, Sable SB, Tripp RA, Kellar KL, Bartlett J, Quinn FD: **An in vitro model of the leukocyte interactions associated with granuloma formation in *Mycobacterium tuberculosis* infection.** *Immunol Cell Biol* 2007, **5**:160–168.
17. Krausgruber T, Blazek K, Smallie T, Alzabin S, Lockstone H, Sahgal N, Hussell T, Feldmann M, Udalova IA: **IRF5 promotes inflammatory macrophage polarization and TH1-TH17 responses.** *Nat Immunol* 2011, **12**:231–238.
18. Satoh T, Takeuchi O, Vandenbon A, Yasuda K, Tanaka Y, Kumagai Y, Miyake T, Matsushita K, Okazaki T, Saitoh T, Honma K, Matsuyama T, Yui K, Tsujimura T, Standley DM, Nakanishi K, Nakai K, Akira S: **The Jmjd3-Irf4 axis regulates M2 macrophage polarization and host responses against helminth infection.** *Nat Immunol* 2010, **11**:936–944.

19. Benoit M, Desnues B, Mege JL: **Macrophage polarization in bacterial infections.** *J Immunol* 2008, **181**:3733–3739.
20. Makino M, Baba M: **A cryopreservation method of human peripheral blood mononuclear cells for efficient production of dendritic cells.** *Scand J Immunol* 1997, **45**:618–622.
21. Maeda Y, Mukai T, Spencer J, Makino M: **Identification of an immunomodulating agent from *Mycobacterium leprae*.** *Infect Immun* 2005, **73**:2744–2750.
22. Levy L, Ji B: **The mouse foot-pad technique for cultivation of *Mycobacterium leprae*.** *Lepr Rev* 2006, **77**:5–24.
23. McDermott-Lancaster RD, Ito T, Kohsaka K, Guelpa-Lauras CC, Grosset JH: **Multiplication of *Mycobacterium leprae* in the nude mouse, and some applications of nude mice to experimental leprosy.** *Int J Lepr Other Mycobact Dis* 1987, **55**:889–895.
24. Hashimoto K, Maeda Y, Kimura H, Suzuki K, Masuda A, Matsuoka M, Makino M: ***Mycobacterium leprae* infection in monocyte-derived dendritic cells and its influence on antigen-presenting function.** *Infect Immun* 2002, **70**:5167–5176.
25. Truman RW, Krahenbuhl JL: **Viable *Mycobacterium leprae* as a research reagent.** *Int J Lepr Other Mycobact Dis* 2001, **69**:1–12.
26. Ridley DS, Jopling WH: **Classification of leprosy according to immunity. A five-group system.** *Int J Lepr Other Mycobact Dis* 1966, **34**:255–273.
27. Hagge DA, Ray NA, Krahenbuhl JL, Adams LB: **An in vitro model for the lepromatous leprosy granuloma: Fate of *Mycobacterium leprae* from target macrophages after interaction with normal and activated effector macrophages.** *J Immunol* 2004, **172**:7771–7779.
28. Kaplan G, Van Voorhis WC, Sarno EN, Nogueira N, Cohn ZA: **The cutaneous infiltrates of leprosy. A transmission electron microscopy study.** *J Exp Med* 1983, **158**:1145–1159.
29. Postlethwaite AE, Jackson BK, Beachey EH, Kang AH: **Formation of multinucleated giant cells from human monocyte precursors. Mediation by a soluble protein from antigen-and mitogen-stimulated lymphocytes.** *J Exp Med* 1982, **155**:168–178.
30. Heuts F, Gavier-Widen D, Carow B, Juarez J, Wigzell H, Rottenberg ME: **CD4+ cell dependent granuloma formation in humanized mice infected with mycobacteria.** *PNAS* 2013, **110**:6482–6487.
31. Laskin DL: **Macrophages and Inflammatory Mediators in Chemical Toxicity: A Battle of Forces.** *Chem Res Toxicol* 2009, **22**:1376–1385.
32. Trujillo G, O'Connor EC, Kunkel SL, Hogaboam CM: **A novel mechanism for CCR4 in the regulation of macrophage activation in bleomycin-induced pulmonary fibrosis.** *Am J Pathol* 2008, **172**:1209–1221.
33. Yamamura M, Wang XH, Ohmen JD, Uyemura K, Rea TH, Bloom BR, Modlin RL: **Cytokine patterns of immunologically mediated tissue damage.** *J Immunol* 1992, **149**:1470–1475.

doi:10.1186/1471-2334-13-279
Cite this article as: Wang *et al.*: **An *in vitro* model of *Mycobacterium leprae* induced granuloma formation.** *BMC Infectious Diseases* 2013 **13**:279.

Infection, Genetics and Evolution 19 (2013) 200–204

Contents lists available at ScienceDirect

Infection, Genetics and Evolution

journal homepage: www.elsevier.com/locate/meegid

Characteristic mutations found in the ML0411 gene of *Mycobacterium leprae* isolated in Northeast Asian countries

M. Kai [a,*], N. Nakata [a], M. Matsuoka [a], T. Sekizuka [b], M. Kuroda [b], M. Makino [a]

[a] Department of Mycobacteriology, Leprosy Research Center, National Institute of Infectious Diseases, 4-2-1 Aoba-cho, Higashimurayama, Tokyo 189-0002, Japan
[b] Pathogen Genomics Center, National Institute of Infectious Diseases, 1-23-1 Toyama, Shinjuku-ku, Tokyo 162-8640, Japan

ARTICLE INFO

Article history:
Received 1 May 2013
Received in revised form 12 July 2013
Accepted 12 July 2013
Available online 24 July 2013

Keywords:
Mycobacterium leprae
Genome
SNPs
Genotyping
Japan

ABSTRACT

Genome analysis of *Mycobacterium leprae* strain Kyoto-2 in this study revealed characteristic nucleotide substitutions in gene ML0411, compared to the reference genome *M. leprae* strain TN. The ML0411 gene of Kyoto-2 had six SNPs compared to that of TN. All SNPs in ML0411 were non-synonymous mutations that result in amino acid replacements. In addition, a seventh SNP was found 41 bp upstream of the start codon in the regulatory region. The seven SNP sites in the ML0411 region were investigated by sequencing in 36 *M. leprae* isolates from the Leprosy Research Center in Japan. The SNP pattern in 14 of the 36 isolates showed similarity to that of Kyoto-2. Determination of the standard SNP types within the 36 stocked isolates revealed that almost all of the Japanese strains belonged to SNP type III, with nucleotide substitutions at position 14676, 164275, and 2935685 of the *M. leprae* TN genome. The geographical distribution pattern of east Asian *M. leprae* isolates by discrimination of ML0411 SNPs was investigated and interestingly turned out to be similar to that of tandem repeat numbers of GACATC in the *rpoT* gene (3 copies or 4 copies), which has been established as a tool for *M. leprae* genotyping. All seven Korean *M. leprae* isolates examined in this study, as well as those derived from Honshu Island of Japan, showed 4 copies of the 6-base tandem repeat plus the ML0411 SNPs observed in *M. leprae* Kyoto-2. They are termed Northeast Asian (NA) strain of *M. leprae*. On the other hand, many of isolates derived from the Okinawa Islands of Japan and from the Philippines showed 3 copies of the 6-base tandem repeat in addition to the *M. leprae* TN ML0411 type of SNPs. These results demonstrate the existence of *M. leprae* strains in Northeast Asian region having characteristic SNP patterns.

1. Introduction

Leprosy is a chronic infectious disease caused by infection with *Mycobacterium leprae*. Dr. Gerhard Hansen, GHA first observed this bacterium in samples derived from leprosy patients in 1873 (Irgens, 1984). At that time, leprosy was prevalent worldwide and the absence of effective drugs for treatment resulted in peripheral nerve damage, leading to severe deformity. Thereafter more effective drugs were used in the treatment of leprosy and deformity was reduced. The present strategy for leprosy treatment is based on the multi-drug therapy (MDT) recommended by the World Health Organization (WHO, 1982), which has successfully reduced the number of leprosy cases in the world (WHO, 2012). However, *M. leprae* cannot be cultivated in artificial medium and the detailed biological characterization of the bacterium still progresses slowly.

Due to advances in molecular biology, the unique characteristics of *M. leprae* are becoming clearer through whole-genome DNA sequencing and analysis. At present, two complete genome sequences of *M. leprae* strains, TN and Br4923, have been determined and are publically accessible on an Internet database (Cole et al., 2001; Monot et al., 2009). The genome size of *M. leprae* is approximately 3.3 Mb, which is smaller than that of *Mycobacterium tuberculosis* (4.4 Mb) (Cole et al., 1998). Massive gene decay was shown within the *M. leprae* genome relative to other mycobacteria and the number of ORFs was estimated at approximately 1600. A previous study using RFLP analysis showed no divergence in *M. leprae* isolate genomes, even when originating from different geographic locations (Clark-Curtiss and Docherty, 1989; Williams et al., 1990). Comparative genome analysis also confirmed the lack of divergence in *M. leprae* isolates. There is no significant difference between whole genomes of the two *M. leprae* strains, TN and Br4923 except SNPs subtyping, although they were isolated from countries that rank among those with the highest leprosy burden, yet are geographically remote (India and Brazil) (Monot et al., 2009). In contrast, single nucleotide polymorphisms (SNPs) and variable number of tandem repeat (VNTR) analysis indicated some

* Corresponding author. Tel.: +81 42 391 8211; fax: +81 42 391 8807.
E-mail addresses: mkai@nih.go.jp (M. Kai), n-nakata@nih.go.jpz (N. Nakata), Matsuoka@nih.go.jp (M. Matsuoka), sekizuka@nih.go.jp (T. Sekizuka), makokuro@nih.go.jp (M. Kuroda), mmaki@nih.go.jp (M. Makino).

1567-1348/$ - see front matter © 2013 Elsevier B.V. All rights reserved.
http://dx.doi.org/10.1016/j.meegid.2013.07.014

variability in the genomic DNA of *M. leprae* isolates (Groathouse et al., 2004; Matsuoka et al., 2004; Monot et al., 2005; Zhang et al., 2005).

M. leprae cannot be cultivated in artificial medium and thus animal models such as the armadillo or athymic nude mice are utilized to grow *M. leprae* bacilli for research. Importantly, the animal models take 1–2 years to establish infection, requiring a great deal of time, manpower, and cost. Moreover, to successfully culture *M. leprae* bacilli from a human biopsy sample, the biopsy materials should be taken from patients who are not undergoing drug treatment. Recently the number of leprosy patients has decreased globally and, although welcomed from a public health perspective, has resulted in a scarcity of biopsy samples for research. The Leprosy Research Center in Japan has established and maintained many *M. leprae* strains over the course of 5 decades (Matsuoka, 2010a,b). We therefore analyzed the genomes of Japanese *M. leprae* strains to identify any small differences as compared with strains TN and Br4923.

2. Materials and methods

2.1. Bacterial strains

M. leprae Thai-53 and Kyoto-2 strains were selected for genome analysis. The Thai-53 strain, derived from an multibacillary (MB) patient in Thailand, has been maintained in the Leprosy Research Center in Japan for a long period upon establishment in the nude mouse footpad system (Kohsaka et al., 1976), and supplied to researchers both foreign and domestic (Matsuoka, 2010b). The Kyoto-2 strain was established from biopsy sample obtained at skin clinic of Kyoto University, Japan (Matsuoka, 2010a). The *M. leprae* strains were passaged in the nude mouse footpad at every 10 months. In addition, a genotyping analysis was undertaken on 34 other isolates, comprised of 17 isolates from the Leprosy Research Center in Japan, 3 isolates from Thailand, 1 isolate from Indonesia, 7 isolates from Korea, and 6 isolates from the Philippines.

2.2. Preparation and sequencing of genomic DNA

Genomic DNA was extracted from the isolates using the QIAamp DNA mini kit (Qiagen). Shotgun DNA libraries were generated according to the manufacturer's sample preparation protocol for genomic DNA (Bentley et al., 2008). Briefly, genomic DNA was randomly sheared. Following ligation of a pair of adaptors to the repaired ends, the DNA was amplified using adaptor primers, and fragments were isolated. Sequencing analysis was done by Illumina GAIIx and reads were mapped to the published complete genome sequence for *M. leprae* strain TN (http://genolist.pasteur.fr/Leproma/). Several gaps were detected and filled in by standard PCR and direct sequencing. The genome sequences of Thai-53 and Kyoto-2 were compared with those of strains TN and Br4923 using Mapview software for genome analysis, with the exception of dispersed repeat regions. In addition, a more limited analysis was done on other strains obtained from collaborators in the Southeast Asian countries.

3. Results

3.1. SNPs analysis

The whole genome sequence, with the exception of the dispersed repeat regions of *M. leprae* Kyoto-2, was determined and compared to that of other *M. leprae* strains. Some peculiar differences, relevant to the Kyoto-2 genome, were found. We focused on one of those interesting differences in the Kyoto-2 genome. The ML0411 gene of Kyoto-2 had six SNPs and five nucleotide differences compared to that of TN and Br4923, respectively. All six SNPs were non-synonymous mutations that result in amino acid replacement. Moreover, one base change was observed at 41 bp

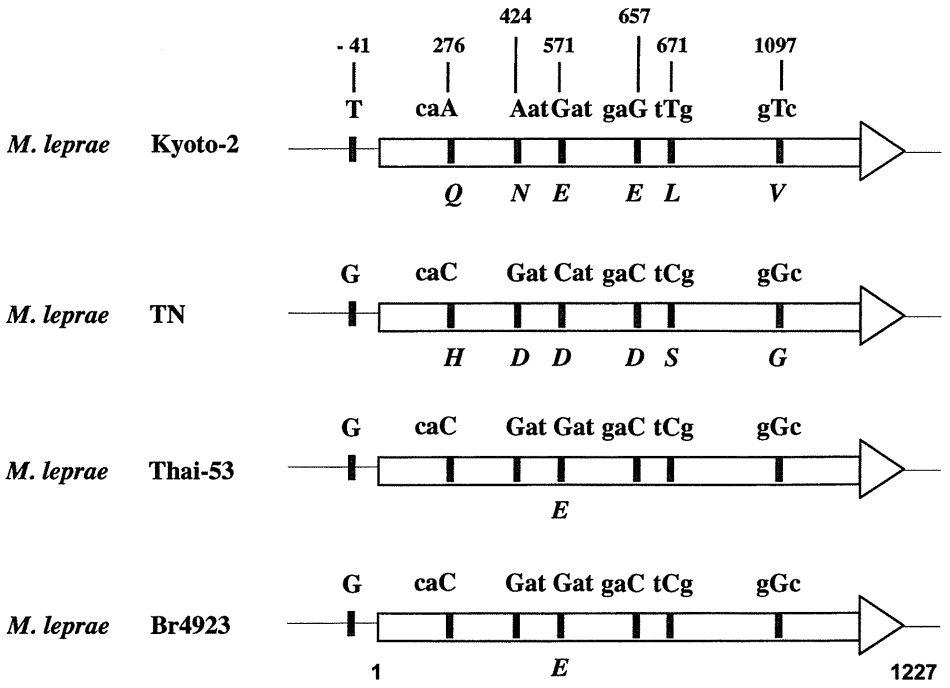

Fig. 1. Comparison of nucleotide sequences of *M. leprae* strains in gene ML0411 and the upstream region. ML0411 gene is indicated with arrows. The letters above arrows show nucleotide bases and set of the three bases indicate codons. SNPs sites of nucleotide bases are indicated with capital letters. The numbers show SNPs position on ML0411. The letters below arrows show amino acids by one letter notation.

upstream of the start codon of ML0411 in the regulatory region (Fig. 1). No other ORF has as many non-synonymous mutations in the *M. leprae* genome. Within the TN and Br4923 strains, there is only one SNP within 191st codon (at position 571st in base sequence) of ML0411.

3.2. Genotyping

The sequences of seven SNP sites in the ML0411 region were investigated in 36 *M. leprae* isolates including Thai-53 and Kyoto-2. The SNP pattern of 19 isolates (12 isolates from Honshu Island in Japan and 7 isolates from Korea) showed a pattern identical to that of Kyoto-2 except at nucleotide 657 (Table 1). On the other hand, all Japanese strains in this study belonged to SNP type III with the exception of one (Airaku-2), that contains a SNP type I involving nucleotides at positions 14676, 164275, and 2935685 of the *M. leprae* TN genome DNA. We compared the standard SNP typing (type I–IV) and the characteristic seven SNPs in Kyoto-2, with the geographical distribution of strains. The results show that isolates having the Kyoto-2 SNP pattern in gene ML0411, including all Korean isolates, were SNP type III, while the other Japanese isolates tested were SNP type III or I. Furthermore, the isolates having the Kyoto-2 SNP pattern turned out to be similar to that of the tandem repeat of six bases (GACATC) in the *rpoT* gene, which has been well-established as a tool for *M. leprae* genotyping. All seven Korean *M. leprae* isolates tested in this study, as well as those 12 isolates derived from Honshu Island in Japan, showed 4 copies of the 6-base tandem repeats. On the other hand, isolates derived from Okinawa Island in Japan and from the Philippines only contained 3 copies of the tandem repeat (Fig. 2).

4. Discussion

Several genetic markers of *M. leprae* have been researched and evaluated for use as epidemiological tools for strain differentiation (Lavania et al., 2007; Matsuoka et al., 2000; Phetsuksiri et al., 2012). SNP typing using nucleotides polymorphisms at three sites of *M. leprae* TN genomic DNA were established (Monot et al., 2005). Four types of SNPs, C-G-A, C-T-A, C-T-C and T-T-C at positions, 14676, 164275, and 2935685 were proposed as Type I–IV in the SNP typing and adopted globally (Sakamuri et al., 2009; Watson and Lockwood, 2009) Recently, a more detailed subtyping system composed of 16 subtypes (subtypes A to P) from 84 SNPs was reported (Monot et al., 2009). Almost all of the Japanese isolates belong to SNP type I or III (Matsuoka, 2010b). The subtypes of the type III Japanese strains, Kyoto-2 and Hoshizuka-4, were determined to be K (unpublished data). Interestingly, six of the unique 7 SNPs in the ML0411 region found in Kyoto-2 (T, A, A, G, T, and T at positions, −41, 276, 424, 571, 671, and 1097, respectively) were not only specific for Kyoto-2 but also for the other Japanese

Table 1
Genotyping of East Asian isolates of *M. leprae* by using several tools.

ML0411								Number of 6bp repeat In *rpoT*	SNPs type (I_IV)	SNPs sub-type (A_P)	Distribution*
Nucleotide position	-41st	276th	424th	571st	657th	671st	1097th				
Amino acid position	–	92nd	142nd	191st	219th	224th	366th				
TN	G	C	G	C	C	C	G	3	I	A	S
Br4923	G	C	G	G	C	C	G	3	IV	P	
Hoshizuka-4	T	A	A	G	C	T	T	4	III	K	N
Kanazawa	T	A	A	G	C	T	T	4	III	ND	
Keifu-4	T	A	A	G	C	T	T	4	III	ND	
Kitasato	T	A	A	G	C	T	T	4	III	ND	
Kusatsu-3	T	A	A	G	C	T	T	4	III	ND	
Kusatsu-6	T	A	A	G	C	T	T	4	III	ND	
Kyoto-1	T	A	A	G	C	T	T	4	III	ND	
Kyoto-2	**T**	**A**	**A**	**G**	**G**	**T**	**T**	**4**	**III**	**K**	
Oku-4	T	A	A	G	C	T	T	4	III	ND	
Tsukuba-1	T	A	A	G	C	T	T	4	III	ND	
Zensho-2	T	A	A	G	C	T	T	4	III	ND	
Zensho-4	T	A	A	G	C	T	T	4	III	ND	
Zensho-5	T	A	A	G	C	T	T	4	III	ND	
Zensho-9	G	C	G	G	C	C	G	3	III	ND	S
Airaku-2	G	C	G	G	C	C	G	3	I	ND	
Airaku-3	G	C	G	G	C	C	G	3	III	ND	
Amami	G	C	G	G	C	C	G	3	III	ND	
Ryukyu-2	G	C	G	G	C	C	G	3	III	ND	
Ryukyu-6	G	C	G	G	C	C	G	3	III	ND	
Thai-53	G	C	G	G	C	C	G	3	I	A	
Thai-237	?	A	?	G	C	C	G	3	I	ND	
Thai-311	G	C	G	G	C	C	G	3	II	ND	
Indonesia	G	C	G	G	C	C	G	3	II	ND	
Korea-1	T	A	A	G	G	T	T	4	III	ND	N
Korea-4	T	A	A	G	C	T	T	4	III	ND	
Korea-5	T	A	A	G	C	T	T	4	III	ND	
Korea-6	T	A	A	G	C	T	T	4	III	ND	
Korea-7	T	A	A	G	C	T	T	4	III	ND	
Korea-8	T	A	A	G	C	T	T	4	III	ND	
Korea-9	T	A	A	G	C	T	T	4	III	ND	
Cebu-1	G	C	G	G	C	C	G	3	II	A	S
Cebu-2	G	C	G	G	C	C	G	3	II	ND	
Cebu-3	G	C	G	G	C	C	G	3	II	A	
Cebu-4	G	C	G	G	C	C	G	3	II	ND	
Cebu-5	G	C	G	G	C	C	G	3	II	ND	
Cebu-6	G	C	G	G	C	C	G	3	II	ND	

* S: type of southern islands of Japan, N: type of Honshu island of Japan.

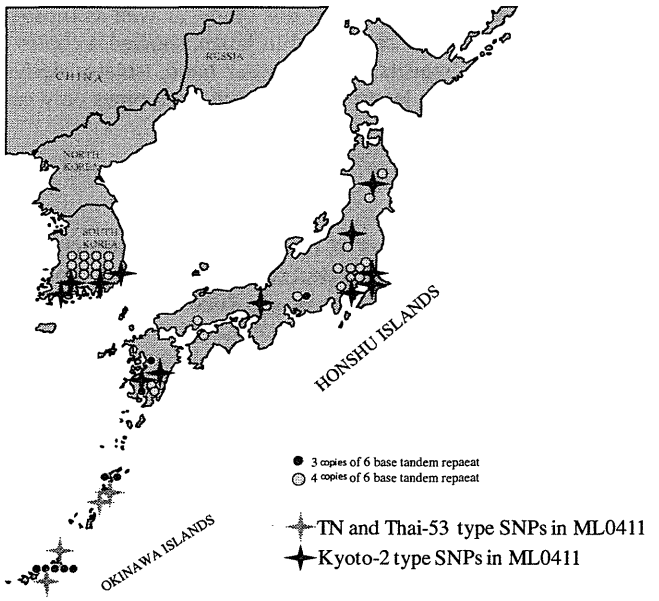

Fig. 2. Geographical distribution of *M. leprae* isolates derived from Japan and Korea having different genotypes.

isolates stocked in the Leprosy Research Center in Japan (Fig. 2). Some isolates derived from areas of the Philippines and Korea geographically nearest to Japan showed that the geographical distributions of the six SNP patterns in ML0411 were divided into two groups: those that contain the Kyoto-2 pattern (T-A-A-G-T-T) including others isolated in Honshu Island of Japan and Korean isolates, or the Thai-53 pattern (G-C-G-C-C-G) including others isolated in the Okinawa Islands of Japan, the Philippines and other southern countries (data not shown). The isolates having the Kyoto-2 SNP pattern in the ML0411 region were SNP type III whereas Thai-53 SNP patterns in the ML0411 region in the other Japanese isolates tested were SNP type I or III. Furthermore, the isolates having the Kyoto-2 SNP pattern turned out to contain 4 copies of the 6-base tandem repeat (GACATC) in the *rpoT* gene, which is well established as a tool for *M. leprae* genotyping (Lavania et al., 2007; Matsuoka et al., 2000). Therefore, these seven SNPs in ML0411 might be useful for studying the geographic distribution of *M. leprae* in the South and East Asian (SA & EA) regions or at a global level. The high frequencies of the standard SNP type I and III and the 3 tandem repeats in *rpoT* are common in SA & EA countries (Matsuoka et al., 2006). The results from this study seem to indicate that some *M. leprae* lineages, showing SNP type III, 4 copies of tandem repeats in *rpoT*, and the Kyoto-2 SNP pattern in ML0411, appear to have disseminated and become established among the people of neighboring and proximal SA & EA countries such as China, Korea and Japan. This linkage might have occurred by genetic linkage in the evolutionary process of *M. leprae*. There has been no report of the existence of such a special lineage in *M. leprae* globally, and these Northeast Asian (NA) strains of *M. leprae* should be further characterized. Recently, *Mycobacterium lepromatosis* was found and established to be closely related to *M. leprae*, but clearly distinct from *M. leprae* (Han et al., 2008; Vera-Cabrera et al., 2011). Although *M. lepromatosis* harbors 4 copies of 6-base tandem repeat in the *rpoT* gene, five nucleotides differ in the flanking region of 6-base tandem repeat and *M. lepromatosis* contains 3 repeats of 21 nucleotides, CGAGCCACCAATACAGCATCT in *rpoT* gene but not *M. leprae*. All NA strains with 4 copies of 6-base tandem repeat in the *rpoT* gene showed identical nucleotide sequences at flanking region of 6-base tandem repeat with *M. leprae* and do not contain 21-base repeats, thus NA strains are clearly belonging to the *M. leprae*. However, here we describe for the first time genotyping by using three indexes, namely, SNPs typing, copy number of 6 base repeats in *rpoT*, and SNPs pattern in ML0411. The grouping of the NA strain is the first report of a strain that has different genotype from that of *M. leprae* strain reported.

The locations of ML0411 and *rpoT* on the *M. leprae* genome are separated by approximately 100 kb. To confirm the possible genetic linkage between ML0411 and *rpoT*, three separate SNPs of the Kyoto-2 genome located between the two genes were selected (coordinates in the *M. leprae* TN genome are 12324, 34353, and 54342) in several *M. leprae* isolates. There was no indication that the SNP pattern can be separated in the Kyoto-2 and TN strains (Fig. S1). The results indicate that there was no genetic linkage between ML0411 and *rpoT*. Therefore, the non-synonymous mutations on ML0411 and variation of copy number of the 6-base tandem repeats in *rpoT* might be evolutionally independent and reflect regional characteristics of *M. leprae* strains. The nucleotide bases of the 191st codon (GAT) in strain TN are changed to CAT in strain Br4923. Combining analysis of the *rpoT* and ML0411 patterns might be useful for identifying not only the NA strain of *M. leprae* but also the detailed genotyping of *M. leprae* strains globally.

Acknowledgments

We thank Drs. G.T. Chae, Institute of Hansen's Disease, Department of Pathology, College of Medicine, The Catholic University of Korea, Seoul, Korea; P. Saunderson, A.A. Maghanoy, and M.F. Balagon, Leonard Wood Memorial, Cebu, The Philippines for supplying DNA samples. Also, we thank Ms. K. Matsubara for her helpful assistance with sequencing. This research was partially supported by a Grant-in-Aid from the Ministry of Education, Culture, Sports, Science and Technology of Japan, and by a Research on Emerging and Re-Emerging Infectious Diseases grant from the Ministry of Health, Labor and Welfare of Japan.

Appendix A. Supplementary data

Supplementary data associated with this article can be found, in the online version, at http://dx.doi.org/10.1016/j.meegid.2013.07.014.

References

Bentley, D.R., Balasubramanian, S., Swerdlow, H.P., Smith, G.P., Milton, J., Brown, C.G., Hall, K.P., Evers, D.J., Barnes, C.L., Bignell, H.R., Boutell, J.M., Bryant, J., Carter, R.J., Keira Cheetham, R., Cox, A.J., Ellis, D.J., Flatbush, M.R., Gormley, N.A., Humphray, S.J., Irving, L.J., Karbelashvili, M.S., Kirk, S.M., Li, H., Liu, X., Maisinger, K.S., Murray, L.J., Obradovic, B., Ost, T., Parkinson, M.L., Pratt, M.R., Rasolonjatovo, I.M., Reed, M.T., Rigatti, R., Rodighiero, C., Ross, M.T., Sabot, A., Sankar, S.V., Scally, A., Schroth, G.P., Smith, M.E., Smith, V.P., Spiridou, A., Torrance, P.E., Tzonev, S.S., Vermaas, E.H., Walter, K., Wu, X., Zhang, L., Alam, M.D., Anastasi, C., Aniebo, I.C., Bailey, D.M., Bancarz, I.R., Banerjee, S., Barbour, S.G., Baybayan, P.A., Benoit, V.A., Benson, K.F., Bevis, C., Black, P.J., Boodhun, A., Brennan, J.S., Bridgham, J.A., Brown, R.C., Brown, A.A., Buermann, D.H., Bundu, A.A., Burrows, J.C., Carter, N.P., Castillo, N., Chiara, E.C.M., Chang, S., Neil Cooley, R., Crake, N.R., Dada, O.O., Diakoumakos, K.D., Dominguez-Fernandez, B., Earnshaw, D.J., Egbujor, U.C., Elmore, D.W., Etchin, S.S., Ewan, M.R., Fedurco, M., Fraser, L.J., Fuentes Fajardo, K.V., Scott Furey, W., George, D., Gietzen, K.J., Goddard, C.P., Golda, G.S., Granieri, P.A., Green, D.E., Gustafson, D.L., Hansen, N.F., Harnish, K., Haudenschild, C.D., Heyer, N.I., Hims, M.M., Ho, J.T., Horgan, A.M., Hoschler, K., Hurwitz, S., Ivanov, D.V., Johnson, M.Q., James, T., Huw Jones, T.A., Kang, G.D., Kerelska, T.H., Kersey, A.D., Khrebtukova, I., Kindwall, A.P., Kingsbury, Z., Kokko-Gonzales, P.I., Kumar, A., Laurent, M.A., Lawley, C.T., Lee, S.E., Lee, X., Liao, A.K., Loch, J.A., Lok, M., Luo, S., Mammen, R.M., Martin, J.W., McCauley, P.G., McNitt, P., Mehta, P., Moon, K.W., Mullens, J.W., Newington, T., Ning, Z., Ling Ng, B., Novo, S.M., O'Neill, M.J., Osborne, M.A., Osnowski, A., Ostadan, O., Paraschos, L.L., Pickering, L., Pike, A.C., Pike, A.C., Chris Pinkard, D., Pliskin, D.P., Podhasky, J., Quijano, V.J., Raczy, C., Rae, V.H., Rawlings, S.R., Chiva Rodriguez, A., Roe, P.M., Rogers, J., Rogert Bacigalupo, M.C., Romanov, N., Romieu, A., Roth, R.K., Rourke, N.J., Ruediger, S.T., Rusman, E., Sanches-Kuiper, R.M., Schenker, M.R., Seoane, J.M., Shaw, R.J., Shiver, M.K., Short, S.W., Sizto, N.L., Sluis, J.P., Smith, M.A., Ernest Sohna Sohna, J., Spence, E.J., Stevens, K., Sutton, N., Szajkowski, L., Tregidgo, C.L., Turcatti, G., Vandevondele, S., Verhovsky, Y., Virk,

S.M., Wakelin, S., Walcott, G.C., Wang, J., Worsley, G.J., Yan, J., Yau, L., Zuerlein, M., Rogers, J., Mullikin, J.C., Hurles, M.E., McCooke, N.J., West, J.S., Oaks, F.L., Lundberg, P.L., Klenerman, D., Durbin, R., Smith, A.J., . Accurate whole human genome sequencing using reversible terminator chemistry. Nature 456, 53–59.

Clark-Curtiss, J.E., Docherty, M.A., 1989. A species-specific repetitive sequence in *Mycobacterium leprae* DNA. J. Infect. Dis. 159, 7–15.

Cole, S.T., Brosch, R., Parkhill, J., Garnier, T., Churcher, C., Harris, D., Gordon, S.V., Eiglmeier, K., Gas, S., Barry 3rd, C.E., Tekaia, F., Badcock, K., Basham, D., Brown, D., Chillingworth, T., Connor, R., Davies, R., Devlin, K., Feltwell, T., Gentles, S., Hamlin, N., Holroyd, S., Hornsby, T., Jagels, K., Krogh, A., McLean, J., Moule, S., Murphy, L., Oliver, K., Osborne, J., Quail, M.A., Rajandream, M.A., Rogers, J., Rutter, S., Seeger, K., Skelton, J., Squares, R., Squares, S., Sulston, J.E., Taylor, K., Whitehead, S., Barrell, B.G., 1998. Deciphering the biology of *Mycobacterium tuberculosis* from the complete genome sequence. Nature 393, 537–544.

Cole, S.T., Eiglmeier, K., Parkhill, J., James, K.D., Thomson, N.R., Wheeler, P.R., Honore, N., Garnier, T., Churcher, C., Harris, D., Mungall, K., Basham, D., Brown, D., Chillingworth, T., Connor, R., Davies, R.M., Devlin, K., Duthoy, S., Feltwell, T., Fraser, A., Hamlin, N., Holroyd, S., Hornsby, T., Jagels, K., Lacroix, C., Maclean, J., Moule, S., Murphy, L., Oliver, K., Quail, M.A., Rajandream, M.A., Rutherford, K.M., Rutter, S., Seeger, K., Simon, S., Simmonds, M., Skelton, J., Squares, R., Squares, S., Stevens, K., Taylor, K., Whitehead, S., Woodward, J.R., Barrell, B.G., 2001. Massive gene decay in the leprosy bacillus. Nature 409, 1007–1011.

Groathouse, N.A., Rivoire, B., Kim, H., Lee, H., Cho, S.N., Brennan, P.J., Vissa, V.D., 2004. Multiple polymorphic loci for molecular typing of strains of *Mycobacterium leprae*. J. Clin. Microbiol. 42, 1666–1672.

Han, X.Y., Seo, Y.H., Sizer, K.C., Schoberle, T., May, G.S., Spencer, J.S., Li, W., Nair, R.G., 2008. A new Mycobacterium species causing diffuse lepromatous leprosy. Am. J. Clin. Pathol. 130, 856–864.

Irgens, L.M., 1984. The discovery of *Mycobacterium leprae*. A medical achievement in the light of evolving scientific methods. Am. J. Dermatopathol. 6, 337–343.

Kohsaka, K., Mori, T., Ito, T., 1976. Lepromatoid lesion developed in the nude mice inoculated with *Mycobacterium leprae*. La Lepro 45, 177–187.

Lavania, M., Katoch, K., Singh, H., Das, R., Gupta, A.K., Sharma, R., Chauhan, D.S., Sharma, V.D., Sachan, P., Sachan, S., Katoch, V.M., 2007. Predominance of three copies of tandem repeats in *rpoT* gene of *Mycobacterium leprae* from Northern India. Infect. Genet. Evol. 7, 627–631.

Matsuoka, M., 2010. The history of *Mycobacterium leprae* Thai-53 strain. Lepr. Rev. 81, 137.

Matsuoka, M., Maeda, S., Kai, M., Nakata, N., Chae, G.T., Gillis, T.P., Kobayashi, K., Izumi, S., Kashiwabara, Y., 2000. *Mycobacterium leprae* typing by genomic diversity and global distribution of genotypes. Int. J. Lepr. Other Mycobacterial Dis.: Official Organ Int. Lepr. Assoc. 68, 121–128.

Matsuoka, M., Zhang, L., Budiawan, T., Saeki, K., Izumi, S., 2004. Genotyping of *Mycobacterium leprae* on the basis of the polymorphism of TTC repeats for analysis of leprosy transmission. J. Clin. Microbiol. 42, 741–745.

Matsuoka, M., Roa, R.I., Budiawan, T., Kyaw, K., Chae, G.T., 2006. Genotypic analysis of *Mycobacterium leprae* isolates from Japan and other Asian countries reveals a global transmission pattern of leprosy. FEMS Microbiol. Lett. 261, 150–154.

Monot, M., Honore, N., Garnier, T., Araoz, R., Coppee, J.Y., Lacroix, C., Sow, S., Spencer, J.S., Truman, R.W., Williams, D.L., Gelber, R., Virmond, M., Flageul, B., Cho, S.N., Ji, B., Paniz-Mondolfi, A., Convit, J., Young, S., Fine, P.E., Rasolofo, V., Brennan, P.J., Cole, S.T., 2005. On the origin of leprosy. Science 308, 1040–1042.

Monot, M., Honore, N., Garnier, T., Zidane, N., Sherafi, D., Paniz-Mondolfi, A., Matsuoka, M., Taylor, G.M., Donoghue, H.D., Bouwman, A., Mays, S., Watson, C., Lockwood, D., Khamesipour, A., Dowlati, Y., Jianping, S., Rea, T.H., Vera-Cabrera, L., Stefani, M.M., Banu, S., Macdonald, M., Sapkota, B.R., Spencer, J.S., Thomas, J., Harshman, K., Singh, P., Busso, P., Gattiker, A., Rougemont, J., Brennan, P.J., Cole, S.T., 2009. Comparative genomic and phylogeographic analysis of *Mycobacterium leprae*. Nat. Genet. 41, 1282–1289.

Phetsuksiri, B., Srisungngam, S., Rudeeaneksin, J., Bunchoo, S., Lukebua, A., Wongtrungkapun, R., Paitoon, S., Sakamuri, R.M., Brennan, P.J., Vissa, V., 2012. SNP genotypes of *Mycobacterium leprae* isolates in Thailand and their combination with rpoT and TTC genotyping for analysis of leprosy distribution and transmission. Jpn J. Infect. Dis. 65, 52–56.

Sakamuri, R.M., Kimura, M., Li, W., Kim, H.C., Lee, H., Kiran, M.D., Black, W.C.t., Balagon, M., Gelber, R., Cho, S.N., Brennan, P.J., Vissa, V., 2009. Population-based molecular epidemiology of leprosy in Cebu, Philippines. J. Clin. Microbiol. 47, 2844–2854.

Vera-Cabrera, L., Escalante-Fuentes, W.G., Gomez-Flores, M., Ocampo-Candiani, J., Busso, P., Singh, P., Cole, S.T., 2011. Case of diffuse lepromatous leprosy associated with "*Mycobacterium lepromatosis*". J. Clin. Microbiol. 49, 4366–4368.

Watson, C.L., Lockwood, D.N., 2009. Single nucleotide polymorphism analysis of European archaeological *M. leprae* DNA. PLoS One 4, e7547.

Who, S.G., 1982. Chemotherapy of leprosy for control programmes. WHO Tech. Rep. Ser. 675, 1–33.

WHO, 2012. Global leprosy situation, 2012. Wkly Epidemiol. Rec. 87, 12.

Williams, D.L., Gillis, T.P., Portaels, F., 1990. Geographically distinct isolates of *Mycobacterium leprae* exhibit no genotypic diversity by restriction fragment length polymorphism analysis. Mol. Microbiol. 4, 1653–1659.

Zhang, L., Budiawan, T., Matsuoka, M., 2005. Diversity of potential short tandem repeats in *Mycobacterium leprae* and application for molecular typing. J. Clin. Microbiol. 43, 5221–5229.

nature immunology

Phosphorylation of the adaptor ASC acts as a molecular switch that controls the formation of speck-like aggregates and inflammasome activity

Hideki Hara[1,5], Kohsuke Tsuchiya[1,5], Ikuo Kawamura[1], Rendong Fang[1], Eduardo Hernandez-Cuellar[1], Yanna Shen[1,2], Junichiro Mizuguchi[3], Edina Schweighoffer[4], Victor Tybulewicz[4] & Masao Mitsuyama[1]

The inflammasome adaptor ASC contributes to innate immunity through the activation of caspase-1. Here we found that signaling pathways dependent on the kinases Syk and Jnk were required for the activation of caspase-1 via the ASC-dependent inflammasomes NLRP3 and AIM2. Inhibition of Syk or Jnk abolished the formation of ASC specks without affecting the interaction of ASC with NLRP3. ASC was phosphorylated during inflammasome activation in a Syk- and Jnk-dependent manner, which suggested that Syk and Jnk are upstream of ASC phosphorylation. Moreover, phosphorylation of Tyr144 in mouse ASC was critical for speck formation and caspase-1 activation. Our results suggest that phosphorylation of ASC controls inflammasome activity through the formation of ASC specks.

Inflammasomes are large multiprotein oligomers that serve critical roles in host defense against microbial pathogens and the development of inflammatory disorders by facilitating the secretion of proinflammatory cytokines[1]. Core components of each inflammasome are pro-caspase-1 and a cytosolic pattern-recognition receptor belonging to the Nod-like receptor (NLR) family or the HIN-200 family, which contains a pyrin domain or a caspase-recruitment domain (CARD). Inflammasome complexes are believed to be assembled after the recognition of specific stimuli by the receptors[2,3]. Once assembled, inflammasomes serve as platforms for the activation of caspase-1, which in turn cleaves the precursor forms of interleukin-1β (IL-1β) and IL-18 to their bioactive forms[4].

Different subsets of inflammasomes are activated by different stimuli. The NLRC4 inflammasome is activated by flagellin and the type III secretion apparatus from bacteria[5–7]. Anthrax lethal toxin produced by *Bacillus anthracis* triggers activation of the NLRP1B inflammasome in mouse macrophages[8]. Activation of the NLRP3 inflammasome depends on a priming step (signal 1) and an activation step (signal 2)[9]. Signal 1 can be induced by signaling via Toll-like receptors, whereas signal 2 is induced by microbial components with diverse molecular structures, such as microbial RNA and toxins[10,11]. In addition, the adjuvant alum and endogenous danger-associated molecules, including ATP and monosodium urate (MSU) crystals, also induce signal 2 for the activation of the NLRP3 inflammasome[10,12,13]. AIM2 and IFI16 sense cytosolic DNA and nuclear DNA, respectively, and DNA viruses[14], *Francisella tularensis*[15], *Listeria monocytogenes*[16,17] and *Streptococcus pneumoniae*[18] have been demonstrated to activate the AIM2 inflammasome or IFI16 inflammasome[19] in host cells.

The adaptor ASC (PYCARD or TMS-1) is composed of a pyrin domain and a CARD and contributes to the assembly of inflammasome complexes[20]. ASC serves as the bridge between pro-caspase-1 and pyrin-containing inflammasomes, such as NLRP3 and AIM2. Accordingly, NLRP3 and AIM2 require ASC exclusively for the recruitment of pro-caspase-1, while the CARD-containing receptors NLRC4 and NLRP1 can directly interact with pro-caspase-1 (refs. 1,7,21). During inflammasome activation, ASC also forms cytosolic macromolecular aggregates of ASC dimers called 'ASC specks', 'ASC foci' or 'pyroptosomes'[22,23]. The ASC speck recruits and activates pro-caspase-1, which leads to the secretion of large amounts of IL-1β and IL-18 and to pyroptosis, a form of programmed cell death. However, ASC is not always essential for cytokine processing and the induction of pyroptosis via the NLRC4 inflammasome. In addition to protein-protein interactions in inflammasome complexes, published reports have revealed the involvement of type I interferons[15,24], the ubiquitin ligase–associated protein SGT1, the heat-shock protein hsp90 (ref. 25), unidentified serine proteases[26] and kinases[27–33], such as PKC-δ, PKR, Syk, Lyn, PI(3)K, Erk and DAPK, in the activation or regulation of inflammasomes, but how these molecules participate in inflammasome activity remains largely unclear.

Given the importance of the protective and pathological roles of inflammasomes, it is worth clarifying what and how signaling factors are involved in the activation of inflammasomes. Here we found that the NLRP3 and AIM2 inflammasomes, but not the NLRC4 inflammasome, required Syk and Jnk for their full activity. Inhibition of Syk or Jnk abolished the NLRP3- or AIM2-mediated formation of ASC specks without affecting the interaction between ASC and NLRP3.

[1]Department of Microbiology, Kyoto University Graduate School of Medicine, Kyoto, Japan. [2]School of Laboratory Medicine, Tianjin Medical University, Tianjin, China. [3]Department of Immunology and Intractable Immunology Research Center, Tokyo Medical University, Tokyo, Japan. [4]MRC National Institute for Medical Research, London, UK. [5]H.H. and K.T. contributed equally to this work. Correspondence should be addressed to M.M. (mituyama@mb.med.kyoto-u.ac.jp).

Received 10 April; accepted 27 September; published online 3 November 2013; doi:10.1038/ni.2749

We also found that ASC underwent Syk- and Jnk-dependent phosphorylation and that Tyr144, one of the possible phosphorylation sites, was critical for speck formation. Our results indicate the phosphorylation of ASC may be an additional target for controlling inflammasome activity.

RESULTS

NLRP3 and AIM2 require Syk and Jnk for IL-18 secretion

To examine the role of kinases in inflammasome activation, we assessed the effects of a series of common kinase inhibitors (**Supplementary Table 1**) on the NLRP3, AIM2 and NLRC4 inflammasomes in peritoneal macrophages. To rule out the possibility of effects of the inhibitors on signal 1 delivered by priming with lipopolysaccharide (LPS), we added the inhibitors to macrophage cultures 3 h after the initiation of LPS priming. Those inhibitors did not affect the abundance of the inflammasome components or of pro-IL-18 or pro-IL-1β at the protein level (**Supplementary Fig. 1a**). We measured IL-18 secretion as an indicator of caspase-1 activation, as pro-IL-18, unlike pro-IL-1β, is constitutively expressed in macrophages[31]. The nigericin-induced secretion of IL-18 from macrophages was significantly lower after pretreatment with an inhibitor of Syk or Jnk, but not after pretreatment with inhibitors of other kinases, than after pretreatment with dimethyl sulfoxide, as a control (**Fig. 1a**). We obtained similar results with mouse bone marrow–derived macrophages and the U937 human macrophage cell line (**Supplementary Fig. 1b,c**), which excluded the possibility of macrophage type– and species-specific effects. The production of IL-18 induced by alum, another NLRP3 activator, was also diminished by pretreatment with an inhibitor of Syk or Jnk (**Supplementary Fig. 1e**), which suggested that Syk and Jnk contributed to activation of the NLRP3 inflammasome. Moreover, we found that the production of IL-18 induced by the synthetic B-form double-stranded DNA poly(dA:dT), but not that induced by flagellin, was substantially inhibited by pretreatment with an inhibitor of Syk or Jnk (**Fig. 1b,c**). To confirm the role of Syk and Jnk in this, we used small interfering RNA to knock down the expression of *Syk* or the genes encoding Jnk1 and Jnk2 (*Mapk8-Mapk9*) in macrophages, and also assessed macrophages with knockout of *Syk*, *Mapk8* or *Mapk9*, and found that either knockdown or knockout decreased the secretion of IL-18 in response to nigericin or poly(dA:dT) (**Fig. 1d–h** and **Supplementary Fig. 2a–d**). Also, the nigericin-induced secretion of IL-1β from macrophages was reduced by an inhibitor of Syk or Jnk or knockout of either *Syk* or *Mapk8-Mapk9* (**Fig. 1e** and **Supplementary Fig. 1d**). Those observations suggested involvement of Syk and Jnk in activation of the NLRP3 and AIM2 inflammasomes. Syk deficiency in macrophages resulted in a moderate decrease in the secretion of IL-18 and IL-1β induced by nigericin (**Fig. 1d,e**), which indicated that Syk was not a critical requirement for activation of the NLRP3 inflammasome but instead contributed to that. *Salmonella enterica* serovar Typhimurium 14028 (*S.* Typhimurium) and *Mycobacterium tuberculosis* strain H37Rv are recognized mainly by NLRC4 and NLRP3, respectively, while *Listeria monocytogenes* strain EGD is recognized by various receptors, including AIM2 and NLRP3 (refs. 6,17,33). Consistent with the results reported above obtained by stimulation by ligands, IL-18 production induced by *S.* Typhimurium was not affected much by inhibition of Syk or Jnk in macrophages, whereas IL-18 production induced by *M. tuberculosis* or *L. monocytogenes* was reduced by inhibition of Syk or Jnk (**Fig. 1i–k**). From these

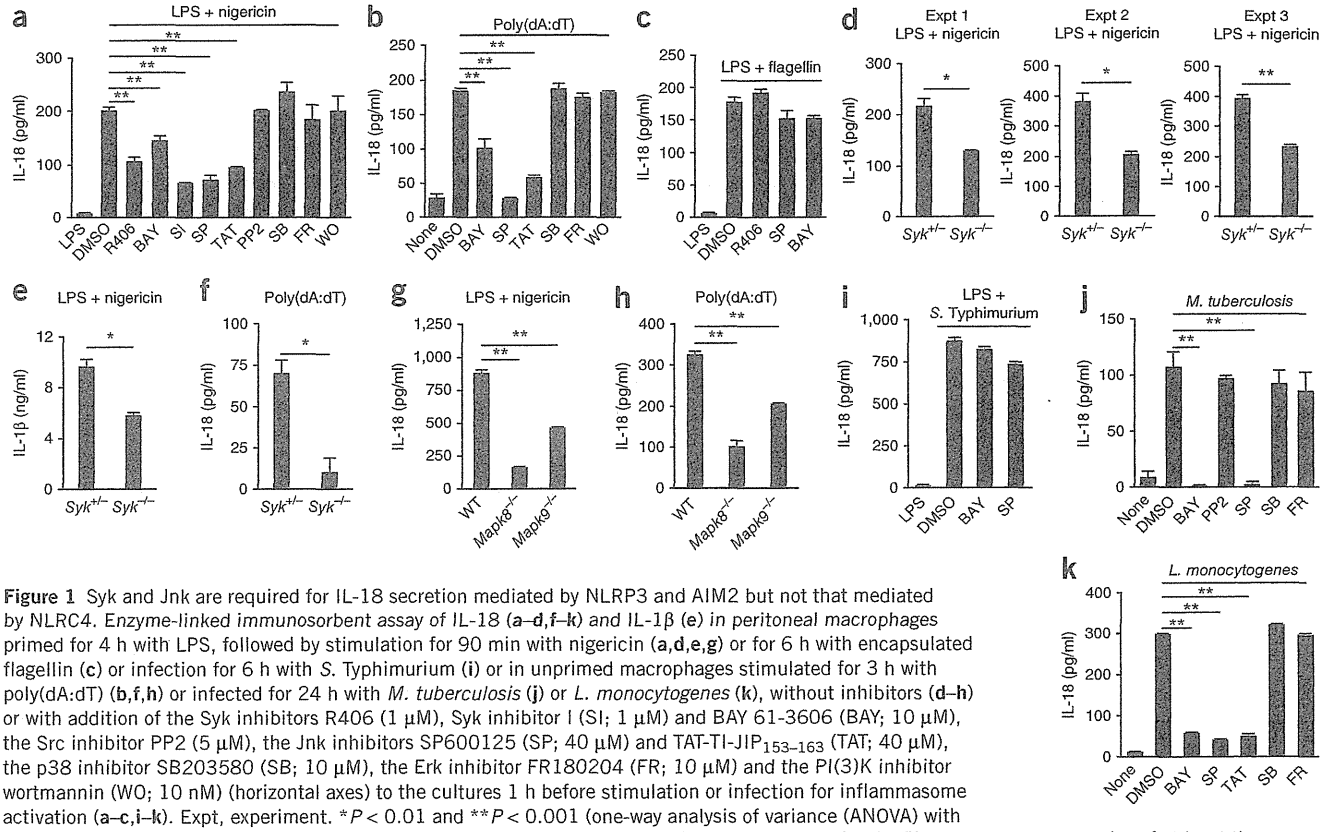

Figure 1 Syk and Jnk are required for IL-18 secretion mediated by NLRP3 and AIM2 but not that mediated by NLRC4. Enzyme-linked immunosorbent assay of IL-18 (**a–d,f–k**) and IL-1β (**e**) in peritoneal macrophages primed for 4 h with LPS, followed by stimulation for 90 min with nigericin (**a,d,e,g**) or for 6 h with encapsulated flagellin (**c**) or infection for 6 h with *S.* Typhimurium (**i**) or in unprimed macrophages stimulated for 3 h with poly(dA:dT) (**b,f,h**) or infected for 24 h with *M. tuberculosis* (**j**) or *L. monocytogenes* (**k**), without inhibitors (**d–h**) or with addition of the Syk inhibitors R406 (1 μM), Syk inhibitor I (SI; 1 μM) and BAY 61-3606 (BAY; 10 μM), the Src inhibitor PP2 (5 μM), the Jnk inhibitors SP600125 (SP; 40 μM) and TAT-TI-JIP$_{153–163}$ (TAT; 40 μM), the p38 inhibitor SB203580 (SB; 10 μM), the Erk inhibitor FR180204 (FR; 10 μM) and the PI(3)K inhibitor wortmannin (WO; 10 nM) (horizontal axes) to the cultures 1 h before stimulation or infection for inflammasome activation (**a–c,i–k**). Expt, experiment. $^*P < 0.01$ and $^{**}P < 0.001$ (one-way analysis of variance (ANOVA) with Bonferroni's multiple-comparison test (**a–c,g–k**) or two-tailed unpaired *t*-test with Welch's correction (**d–f**)). Data are representative of at least three independent experiments (**a–f,i–k**) or two independent experiments (**g,h**; mean and s.d. of triplicates).

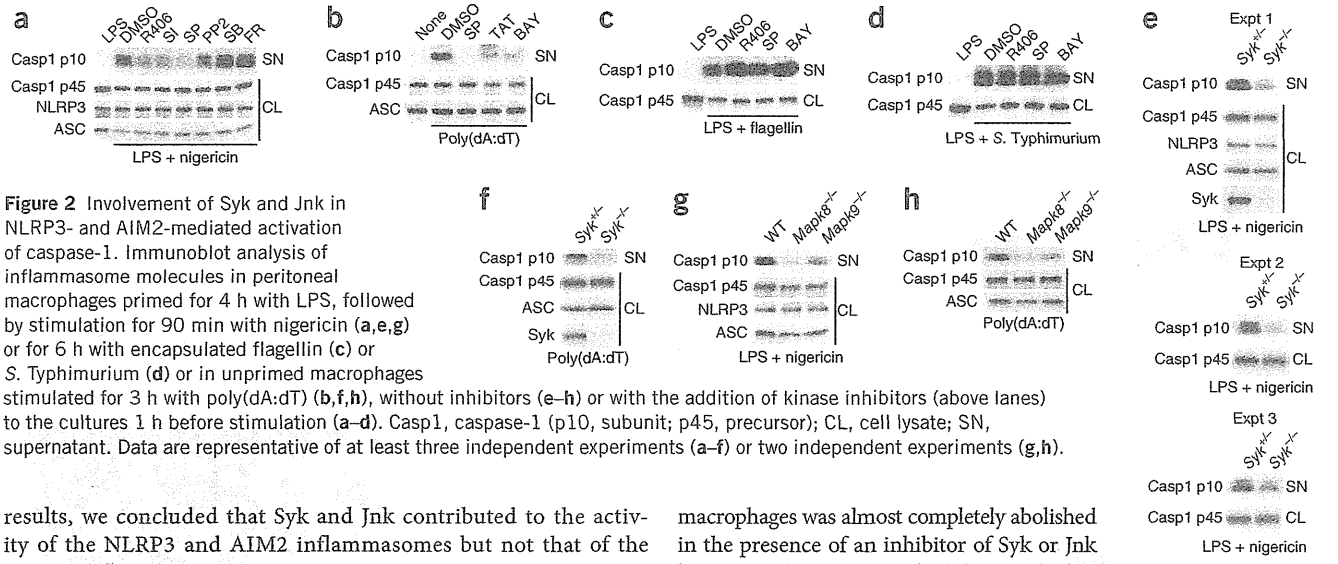

Figure 2 Involvement of Syk and Jnk in NLRP3- and AIM2-mediated activation of caspase-1. Immunoblot analysis of inflammasome molecules in peritoneal macrophages primed for 4 h with LPS, followed by stimulation for 90 min with nigericin (**a**,**e**,**g**) or for 6 h with encapsulated flagellin (**c**) or *S.* Typhimurium (**d**) or in unprimed macrophages stimulated for 3 h with poly(dA:dT) (**b**,**f**,**h**), without inhibitors (**e**–**h**) or with the addition of kinase inhibitors (above lanes) to the cultures 1 h before stimulation (**a**–**d**). Casp1, caspase-1 (p10, subunit; p45, precursor); CL, cell lysate; SN, supernatant. Data are representative of at least three independent experiments (**a**–**f**) or two independent experiments (**g**,**h**).

results, we concluded that Syk and Jnk contributed to the activity of the NLRP3 and AIM2 inflammasomes but not that of the NLRC4 inflammasome.

Caspase-1 activation requires Syk and Jnk

Next we assessed the involvement of Syk and Jnk in the activation of caspase-1 via the NLRP3 and AIM2 inflammasomes. Activation of caspase-1 induced by nigericin, alum or poly(dA:dT) in peritoneal macrophages was almost completely abolished in the presence of an inhibitor of Syk or Jnk but not in the presence of inhibitors of other kinases (**Fig. 2a,b** and **Supplementary Fig. 1f**). In contrast, we did not observe effects of those two inhibitors on the activation of caspase-1 induced by flagellin or *S.* Typhimurium (**Fig. 2c,d**). Furthermore, activation of caspase-1 induced by nigericin or poly(dA:dT) was reduced in Syk- or Jnk-deficient macrophages and by knockdown of those kinases

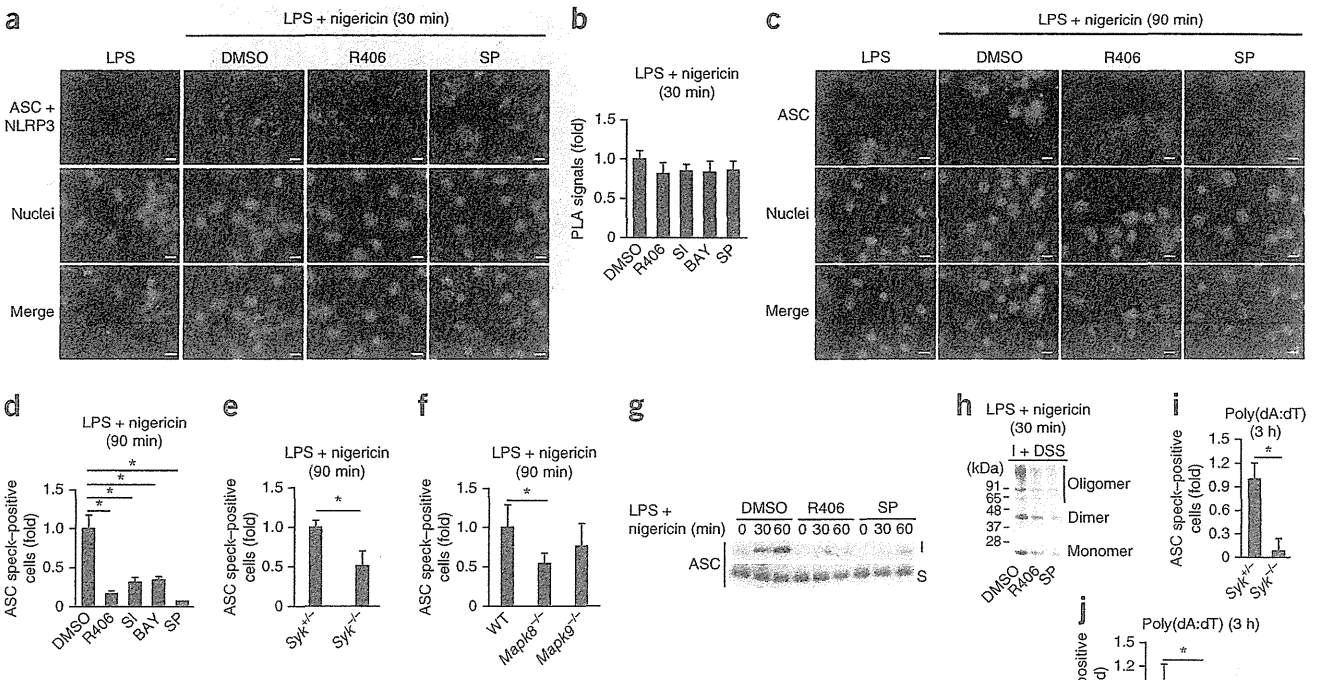

Figure 3 Requirement for signaling via Syk and Jnk for ASC aggregation. (**a**–**h**) *In situ* PLA of ASC-NLRP3 complexes (**a**,**b**), ASC staining (**c**–**f**) and immunoblot analysis of ASC (**g**,**h**) in peritoneal macrophages primed for 4 h with LPS, followed by stimulation for various times (above) with nigericin in the presence or absence of kinase inhibitors. (**a**,**c**) ASC-NLRP3 complexes, red (**a**); ASC, green (**c**); nuclei, blue (**a**,**c**). Scale bars, 10 μm. (**b**) Quantification of PLA signals per cell, presented relative to that of control cells treated with solvent. (**d**–**f**) Quantification of cells with ASC specks, presented relative to that of control cells treated with solvent or wild-type cells. (**g**,**h**) Triton-soluble (S) and Triton-insoluble (I) fractions (right margin; **g**) or Triton-insoluble fractions treated with disuccinimidyl suberate (I + DSS; **h**). (**i**,**j**) ASC staining in unprimed macrophages stimulated for 3 h with poly(dA:dT), presented as in **d**–**f**. *$P < 0.001$ (Kruskal-Wallis test with Dunn's multiple-comparison test (**b**,**j**), one-way ANOVA with Bonferroni's multiple-comparison test (**d**,**f**), two-tailed unpaired *t*-test with Welch's correction (**e**) or Mann-Whitney test (**i**)). Data are representative of at least three independent experiments (**a**–**d**,**g**,**h**) or two independent experiments (**e**,**f**,**i**,**j**; mean and s.d. of triplicates in **b**,**d**–**f**,**i**,**j**).

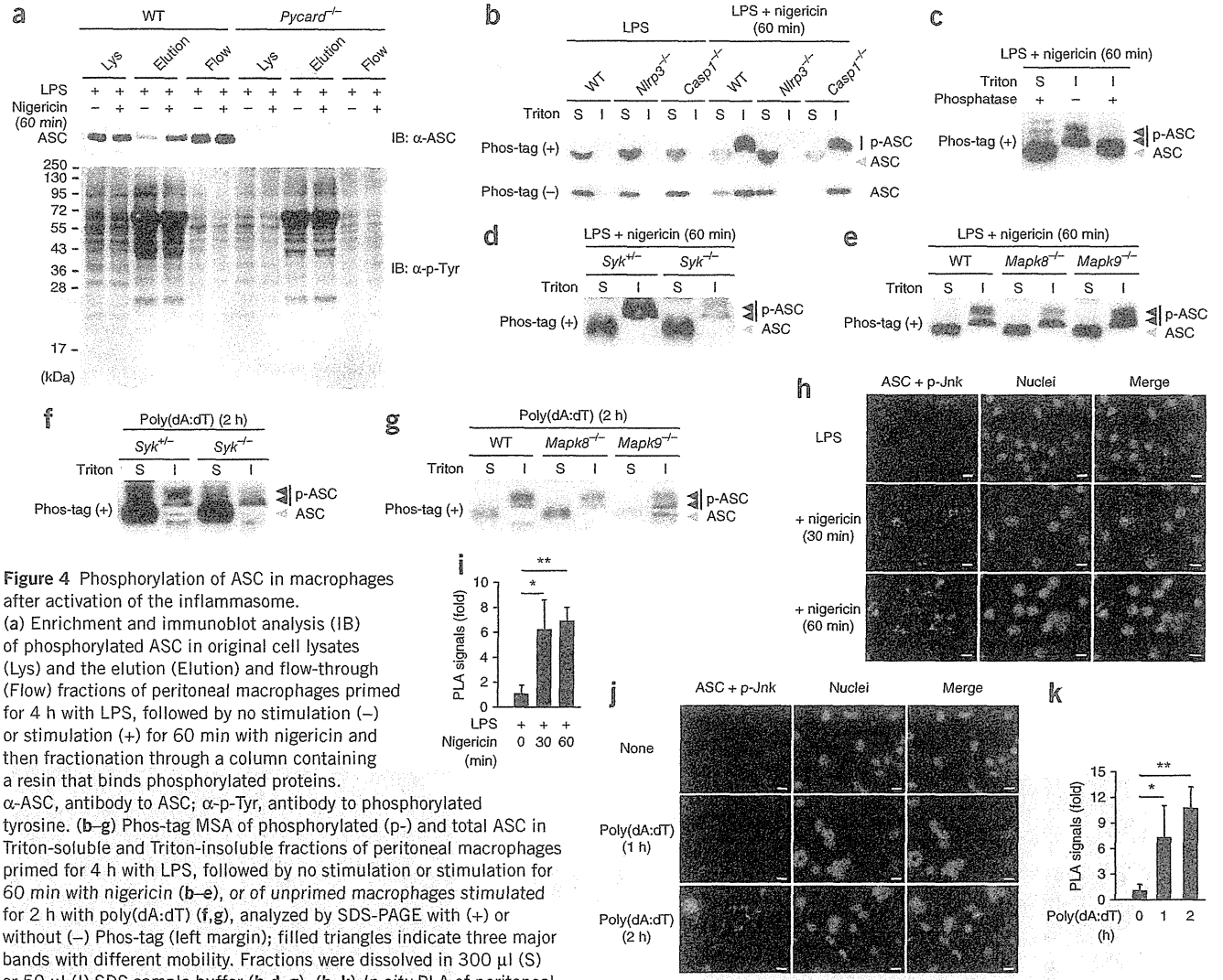

Figure 4 Phosphorylation of ASC in macrophages after activation of the inflammasome. (**a**) Enrichment and immunoblot analysis (IB) of phosphorylated ASC in original cell lysates (Lys) and the elution (Elution) and flow-through (Flow) fractions of peritoneal macrophages primed for 4 h with LPS, followed by no stimulation (−) or stimulation (+) for 60 min with nigericin and then fractionation through a column containing a resin that binds phosphorylated proteins. α-ASC, antibody to ASC; α-p-Tyr, antibody to phosphorylated tyrosine. (**b–g**) Phos-tag MSA of phosphorylated (p-) and total ASC in Triton-soluble and Triton-insoluble fractions of peritoneal macrophages primed for 4 h with LPS, followed by no stimulation or stimulation for 60 min with nigericin (**b–e**), or of unprimed macrophages stimulated for 2 h with poly(dA:dT) (**f,g**), analyzed by SDS-PAGE with (+) or without (−) Phos-tag (left margin); filled triangles indicate three major bands with different mobility. Fractions were dissolved in 300 μl (S) or 50 μl (I) SDS sample buffer (**b,d–g**). (**h–k**) *In situ* PLA of peritoneal macrophages primed for 4 h with LPS, followed by stimulation for 0–60 min with nigericin (**h,i**) or of unprimed macrophages stimulated for 0–2 h with poly(dA:dT) (**j,k**). (**h,j**) Red, complexes of ASC with phosphorylated Jnk (ASC + p-Jnk); blue, nuclei. Scale bars, 10 μm. (**i,k**) Results presented relative to those of unstimulated control cells. $^{*}P < 0.01$ and $^{**}P < 0.001$ (Kruskal-Wallis test with Dunn's multiple-comparison test (**i**) or one-way ANOVA with Tukey-Kramer multiple-comparison test (**k**)). Data are representative of two (**a,c,e–g**) or three (**b,d,h–k**) independent experiments (mean and s.d. of triplicates in **i,k**).

mediated by small interfering RNA (**Fig. 2e–h** and **Supplementary Fig. 2e,f**). The activation of caspase-1 induced by *M. tuberculosis* or *L. monocytogenes* in macrophages was lower after treatment with an inhibitor Syk or Jnk than after treatment with the dimethyl sulfoxide control (data not shown). These results suggested that Syk and Jnk signals were involved in the activation of caspase-1 through the NLRP3 and AIM2 inflammasomes but not in the NLRC4 inflammasome-dependent activation of caspase-1.

Syk is not required for NLRP3 inflammasome in dendritic cells

It has been reported that Syk is not required for nigericin-induced activation of the NLRP3 inflammasome in dendritic cells[28]. Consistent with that report, we observed no significant difference between wild-type and Syk-deficient bone marrow–derived dendritic cells in caspase-1 activation or IL-18 secretion in response to nigericin (**Supplementary Fig. 3a,c,d**). In contrast, IL-18 secretion and caspase-1 activation induced by nigericin were lower in Syk-deficient peritoneal macrophages and bone marrow–derived macrophages than in $Syk^{+/+}$ or $Syk^{+/-}$ cells (**Figs. 1d,e** and **2e** and **Supplementary Fig. 3b,e**). This suggested that the requirement for Syk in NLRP3 activation in response to nigericin was cell type specific.

Syk and Jnk regulate inflammasomes via unknown pathways

We investigated whether inflammasome-activating agents induced activation of Syk and Jnk, assessed by the detection of phosphorylated kinases. Stimulation with nigericin or poly(dA:dT) induced detectable levels of phosphorylated Syk and Jnk (**Supplementary Fig. 4a–d**). The phosphorylation of Jnk induced by nigericin or poly(dA:dT) was not reduced by inhibitors of Syk or in Syk-deficient peritoneal macrophages (**Supplementary Fig. 4e–g**), which suggested that Syk is not upstream of Jnk in this process. Syk is reported to serve a pivotal role in activation of the NLRP3 inflammasome in response to *Candida albicans* by inducing the generation of reactive oxygen species (ROS) and CARD9-dependent activation of the transcription factor NF-κB[28]. However, we

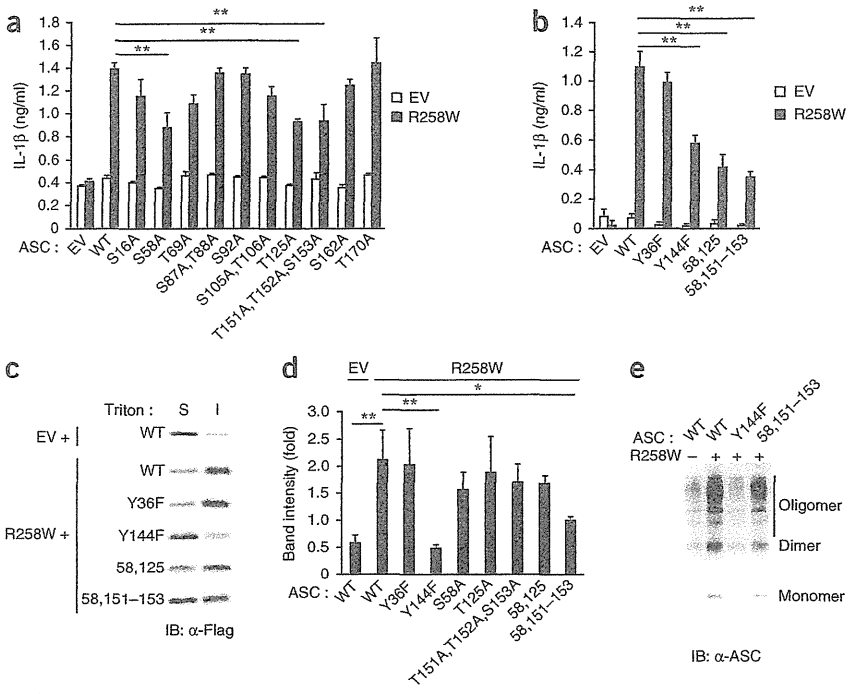

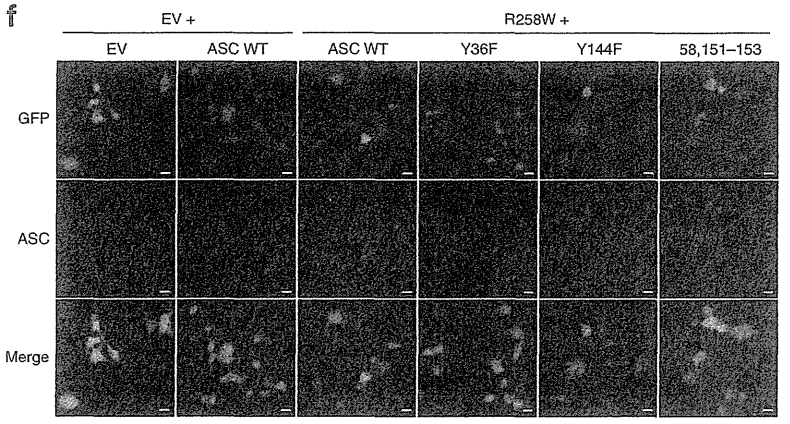

Figure 5 Identification of amino acid residues in ASC critical for its biological activities. (**a**,**b**) Enzyme-linked immunosorbent assay of IL-1β in HEK293 cells 48 h after reconstitution by transfection of empty vector (EV) or vector encoding Flag-tagged NLRP3(R258W) (100 ng) (key) along with empty vector or vector encoding Flag-tagged wild-type (WT) or mutant ASC (10 ng; horizontal axes), plus vector encoding pro-caspase-1 (30 ng) and pro-IL-1β (100 ng). 58,125, ASC(S58A) with the additional substitution T125A. (**c**–**e**) Immunoblot analysis (**c**,**e**) and quantification (**d**) of ASC in Triton-soluble and Triton-insoluble fractions (**c**,**d**) and disuccinimidyl suberate–treated Triton-insoluble fractions (**e**) of reconstituted HEK293 cells 48 h after transfection of empty vector or vector encoding Flag-tagged NLRP3(R258W) (left margin (**c**), top (**d**) or above lanes (**e**)) along with vector encoding Flag-tagged wild-type or mutant ASC (left margin (**c**), horizontal axis (**d**) or above lanes (**e**)); in **d**, band intensity of insoluble ASC is presented relative to that of soluble ASC. (**f**) ASC staining in HEK293 cells treated as in **c**–**e**: red, ASC; green, transfected cells (visualized by transfection of a plasmid encoding green fluorescent protein (100 ng)). Scale bars, 10 μm. $*P < 0.05$ and $**P < 0.001$ (one-way ANOVA with Bonferroni's multiple-comparison test (**a**,**b**) or Tukey-Kramer's multiple-comparison test (**d**)). Data are from one experiment representative of three independent experiments (mean and s.d. of triplicates in **a**,**b**,**d**).

observed that wild-type and CARD9-deficient macrophages produced similar levels of IL-18 in response to nigericin or poly(dA:dT) and that the ROS scavenger BHA did not affect activation of the AIM2 inflammasome in macrophages (**Supplementary Fig. 4h–j**). Moreover, the expression of mitochondrial ROS, which is important for the activation of NLRP3, was not reduced by an inhibitor of Syk or Jnk in nigericin-stimulated macrophages (**Supplementary Fig. 4k**). These results indicated that Syk- and Jnk-dependent activation of the inflammasome is not mediated by ROS or CARD9 and that Syk and Jnk operate in a different pathway(s).

The formation of ASC specks requires Syk and Jnk

Both NLRP3 and AIM2 require the common adaptor ASC to recruit and activate pro-caspase-1 (ref. 1). We therefore speculated that Syk and Jnk might be involved in the interaction of ASC with NLRP3 or AIM2. To investigate that possibility, we visualized ASC-NLRP3 complexes by an *in situ* proximity ligation assay (PLA). As reported before[30], we observed small spots of ASC-NLRP3 complexes in peritoneal macrophages, and these increased in abundance after stimulation with nigericin (**Fig. 3a**). The abundance of spots was not increased by stimulation with nigericin in the absence of ASC or NLRP3 (data not shown), which suggested that ASC-NLRP3 complexes were specifically visualized by this technique. After stimulation with nigericin, the number of spots representing ASC-NLRP3 complexes was similar in macrophages pretreated with an inhibitor of Syk or Jnk and those pretreated with dimethyl sulfoxide (**Fig. 3a**,**b**), which indicated that inhibition of Syk or Jnk did not affect the interaction between NLRP3 and ASC, a critical step in formation of the NLRP3 inflammasome, in macrophages stimulated with nigericin. Next we visualized the formation of ASC specks and found that pretreatment with an inhibitor of Syk or Jnk or deficiency in either Syk or Jnk reduced the nigericin-induced formation of ASC specks in macrophages (**Fig. 3c–f** and **Supplementary Fig. 5a**,**b**). Because ASC has been reported to form Triton X-100–resistant aggregates[20], we prepared Triton X-100–soluble and Triton X-100–insoluble fractions from macrophages to analyze the distribution of ASC. ASC was almost undetectable in the Triton X-100–insoluble fraction of LPS-primed macrophages but was significantly greater in abundance after stimulation with nigericin (**Fig. 3g**). Moreover, most ASC in the Triton X-100–insoluble fraction was a dimer or oligomer[15] (**Fig. 3h**). Pretreatment with an inhibitor of Syk or Jnk reduced the redistribution of ASC induced by nigericin and also resulted in a decrease in the amount of dimerized and oligomerized ASC (**Fig. 3g**,**h**). We obtained similar results for macrophages stimulated with poly(dA:dT) (**Fig. 3i**,**j** and **Supplementary Fig. 5c–f**). These results suggested that signaling by Syk and Jnk was required for the formation of ASC specks but not for the NLR-ASC interaction.

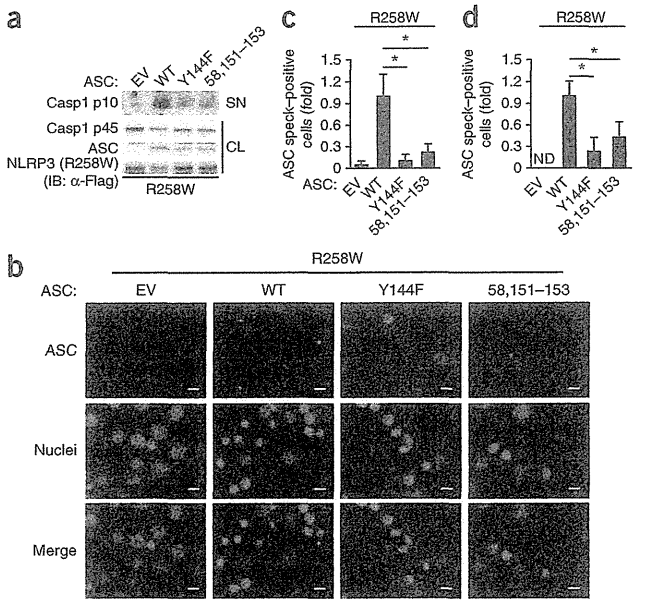

Figure 6 Critical roles of the possible phosphorylation sites of ASC in macrophages. (**a–c**) Immunoblot analysis of inflammasome molecules (**a**), ASC staining (**b**) and quantification of ASC specks (**c**) in reconstituted RAW264.7 cells 9 h after transfection of vector encoding Flag-tagged NLRP3(R258W) plus empty vector or vector encoding wild-type or mutant ASC (above lanes or images (**a**,**b**) or horizontal axis (**c**)). (**b**) ASC, green; nuclei, blue. Scale bars, 10 μm. (**c**) Results presented relative to those of the cells transfected with empty vector. (**d**) Quantification of ASC specks in primary *Pycard*$^{-/-}$ peritoneal macrophages 9 h after reconstitution by transfection of vector encoding Flag-tagged NLRP3(R258W) plus empty vector or vector encoding Flag-tagged ASC (presented as in **c**). ND, not detected. $^{*}P < 0.001$ (one-way ANOVA with Bonferroni's multiple-comparison test (**c**,**d**)). Data are from one experiment representative of three independent experiments (mean and s.d. of triplicates in **c**,**d**).

Phosphorylation of ASC after inflammasome activation

A published report has implied that ASC undergoes phosphorylation in response to inflammatory stimuli[34]. To investigate whether the aggregate formation of ASC was regulated by its phosphorylation mediated by Syk and Jnk during inflammasome activation, we enriched phosphorylated proteins from macrophage lysates through the use of a column containing a phosphorylated protein–binding resin and then detected ASC by immunoblot analysis. We observed that stimulation with nigericin induced an increase in the amount of ASC in the elution fraction (with enrichment for phosphorylated proteins; **Fig. 4a**). To further analyze the phosphorylation of ASC, we obtained Triton X-100–soluble and Triton X-100–insoluble cell lysates and analyzed them by a mobility-shift assay (MSA) based on the phosphate-binding tag Phos-tag[35]. In these gels, ASC in the Triton X-100–insoluble fraction migrated more slowly than that in the Triton X-100–soluble fraction, and the shift in mobility was reversed by phosphatase treatment (**Fig. 4b,c**), which suggested that ASC in the former fraction was phosphorylated. We observed the slowly migrating ASC in the Triton X-100–insoluble fraction of caspase-1-deficient macrophages but not in that of NLRP3-deficient macrophages, after stimulation with nigericin (**Fig. 4b**), which suggested that the increase in phosphorylated ASC in response to nigericin required NLRP3 but not caspase-1. ASC may be phosphorylated at multiple sites, as we detected three major bands with different mobility (**Fig. 4c–g**).

In addition, deficiency in either Syk or Jnk decreased the intensity of the ASC band with the lowest mobility in the Triton X-100–insoluble fraction of macrophages stimulated with nigericin or poly(dA:dT) (**Fig. 4d–g**). We obtained similar results with an inhibitor of Syk or Jnk (data not shown). These data suggested that ASC was phosphorylated after activation of the NLRP3 and AIM2 inflammasomes via the Syk and Jnk pathways. Syk and DAPK have been shown to associate with the NLRP3 inflammasome complex[29,30]. Accordingly, we analyzed the interaction of ASC with phosphorylated Jnk by *in situ* PLA. We observed complexes of ASC with phosphorylated Jnk in wild-type macrophages (**Fig. 4h–k**), but not in ASC-deficient macrophages (negative control; data not shown), after stimulation with nigericin or poly(dA:dT). Notably, most of the complexes were located in or around the nucleus at later time points (**Fig. 4h,j**). These data suggested that ASC was phosphorylated after activation of the NLRP3 and AIM2 inflammasomes via the Syk and Jnk pathways.

Phosphorylation of ASC is critical for inflammasome activation

We next sought to identify ASC-phosphorylation sites that regulate the aggregate formation that results in activation of caspase-1. We detected 14 or 8 possible phosphorylation sites, respectively, in mouse ASC with NetPhos (a neural network–based method for predicting potential phosphorylation sites at serine, threonine or tyrosine residues; version 2.0), at a threshold of 0.5, or with GPS (a group-based prediction system for the computational prediction of phosphorylation sites with their cognate kinases; version 2.1.1) with the low threshold (**Supplementary Fig. 6** and **Supplementary Table 2**). We constructed a series of expression vectors encoding ASC

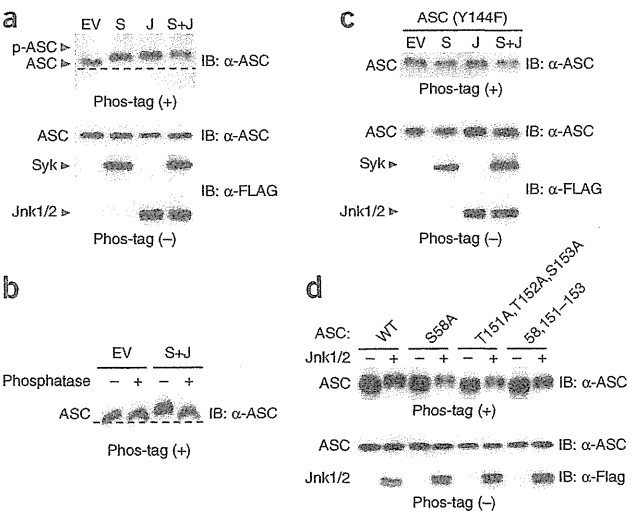

Figure 7 Identification of phosphorylation sites in ASC. (**a**) Phos-tag MSA of reconstituted HEK293 cells 48 h after transfection of vector encoding Flag-tagged wild-type ASC (50 ng) plus empty vector or vector encoding Syk (300 ng) (S) or Jnk1 (300 ng) and Jnk2 (300 ng) (J) or vectors encoding Syk, Jnk1 and Jnk2 (S+J). (**b**) Phos-tag MSA of reconstituted HEK293 cells 48 h after transfection of vector encoding Flag-tagged wild-type ASC plus empty vector or vectors encoding Syk, Jnk1 and Jnk2, followed by no treatment (–) or treatment with phosphatase (+). (**c**) Phos-tag MSA of reconstituted HEK293 cells 48 h after transfection of vector encoding Flag-tagged ASC(Y144F) plus vectors as in **a** (above lanes). (**d**) Phos-tag MSA of reconstituted HEK293 cells 48 h after transfection of vector encoding Flag-tagged wild-type or mutant ASC (top) plus empty vector (–) or vector Jnk1 (300 ng) and Jnk2 (300 ng) (+). Data are representative of three independent experiments.

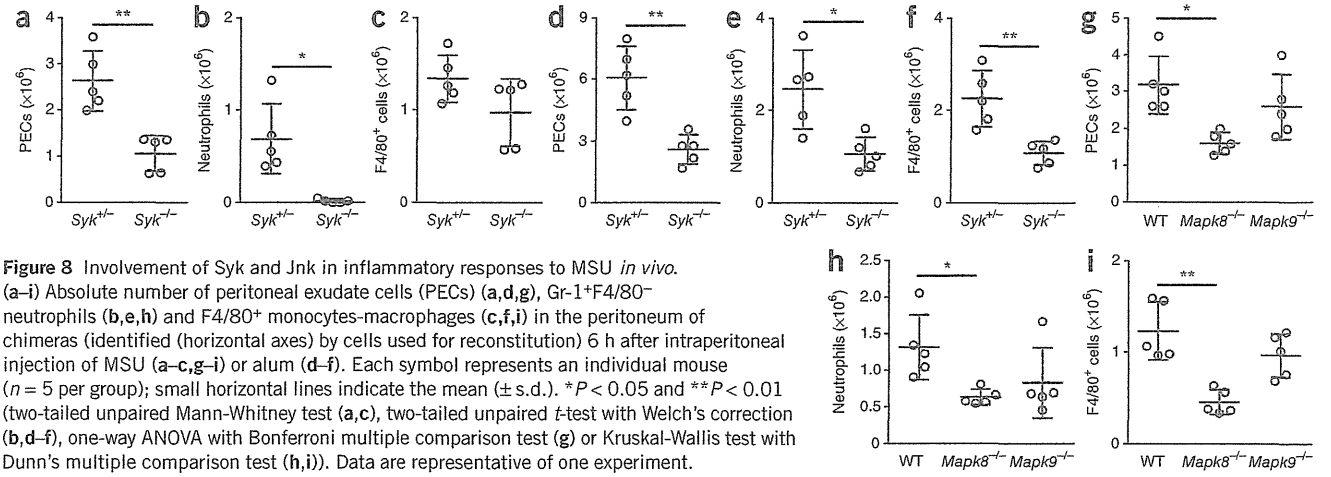

Figure 8 Involvement of Syk and Jnk in inflammatory responses to MSU *in vivo*. (**a–i**) Absolute number of peritoneal exudate cells (PECs) (**a**,**d**,**g**), Gr-1$^+$F4/80$^-$ neutrophils (**b**,**e**,**h**) and F4/80$^+$ monocytes-macrophages (**c**,**f**,**i**) in the peritoneum of chimeras (identified (horizontal axes) by cells used for reconstitution) 6 h after intraperitoneal injection of MSU (**a–c**,**g–i**) or alum (**d–f**). Each symbol represents an individual mouse ($n = 5$ per group); small horizontal lines indicate the mean (± s.d.). $^*P < 0.05$ and $^{**}P < 0.01$ (two-tailed unpaired Mann-Whitney test (**a**,**c**), two-tailed unpaired *t*-test with Welch's correction (**b**,**d–f**), one-way ANOVA with Bonferroni multiple comparison test (**g**) or Kruskal-Wallis test with Dunn's multiple comparison test (**h**,**i**)). Data are representative of one experiment.

mutants in which amino acid residues predicted to be phosphorylated were replaced with alanine or phenylalanine, then assessed the ability of those ASC point mutants to induce IL-1β secretion in an inflammasome-reconstitution system based on HEK293 human embryonic kidney cells (**Supplementary Fig. 7a,b**). We observed that the ability of the point mutants ASC(S58A), ASC(T125A), ASC(Y144F) or ASC(T151A,T152A,S153A) to induce IL-1β secretion in response to NLRP3(R258W), a disease-associated mutant of NLRP3, was slightly lower that of wild-type ASC (**Fig. 5a,b**). We further altered the ASC(S58A) mutant by the additional substitution T125A or with the three additional substitutions of T151A, T152A and S153A (ASC(58,151–153)) and found that IL-1β-inducing ability of the resulting ASC mutants was significantly lower than that of ASC(S58A) (**Fig. 5b**). Furthermore, ASC(Y144F) and ASC(58,151–153) showed less redistribution into the Triton X-100–insoluble fraction in response to NLRP3(R258W) than did wild-type ASC (**Fig. 5c,d**). ASC(Y144F) and ASC(58,151–153) were still able to form dimers and oligomers in the Triton X-100–insoluble fraction (**Fig. 5e**), probably because those substitutions affected the redistribution of ASC without affecting its dimerization or oligomerization. Moreover, we found that ASC(Y144F) expressed together with NLRP3(R258W) formed almost no aggregates, in contrast to wild-type ASC expressed together with NLRP3(R258W) (**Fig. 5f**). These results suggested that Tyr144, Ser58, Thr151, Thr152 and Ser153, all putative phosphorylation sites of ASC, were involved in both IL-1β-inducing ability and aggregate formation.

We investigated whether those results obtained with HEK293 cell could be reproduced in the mouse macrophage cell line RAW264.7, which lacks ASC expression. Wild-type ASC expressed together with NLRP3(R258W) in RAW264.7 cells formed speck-like structures and induced the activation of caspase-1, whereas speck formation was diminished in RAW264.7 cells transfected to express ASC(Y144F) or ASC(58,151–153) (**Fig. 6a–c**). The formation of ASC specks was also abrogated by the substitutions in similar experiments with ASC-deficient primary macrophages (**Fig. 6d**).

We further investigated whether those residues were phosphorylated in a Syk- and Jnk-dependent manner. ASC expressed together with either Syk or Jnk migrated more slowly in Phos-tag gels than did ASC in cells transfected with empty vector (**Fig. 7a**). Transfection of cells to express ASC with both Syk and Jnk resulted in a greater mobility shift, which was reversed by phosphatase treatment (**Fig. 7a,b**). These results suggested that ASC was phosphorylated at multiple sites in a Syk- and Jnk-dependent manner. The observed changes in the mobility of ASC in the presence of Syk or Jnk were all abrogated by the Y144F substitution in ASC (**Fig. 7c**). In contrast, the mobility of ASC(S58A), ASC(T151A,T152A,S153A) and ASC(58,151–153) in Phos-tag gels, like that of wild-type ASC, was reduced by overexpression of Jnk1-Jnk2 (**Fig. 7d**), which suggested that Ser58, Thr151, Thr152 and Ser153 were not phosphorylated in a Jnk-dependent manner or that the effect of those substitutions on the mobility may have been masked by phosphorylation at other residues. These results showed that phosphorylation of Tyr144 was required for inflammasome activation.

We did *in vitro* kinase assays with synthetic peptides (amino acids 139–150 of mouse ASC or amino acids 141–152 of human ASC) to investigate the possibility that Syk directly phosphorylates Tyr144 of mouse ASC and the corresponding tyrosine residue of human ASC. We incubated those peptides with ATP in the presence or absence of recombinant Syk and assessed the kinase reaction by the consumption of ATP. We did not observe substantially less ATP in reactions in which we used those ASC peptides as a substrate for recombinant Syk, whereas reactions containing purified tubulin, as a positive control substrate, had less ATP (data not show). Thus, our data did not support or were not sufficient to justify the possibility of direct phosphorylation of Tyr144 by Syk.

MSU- and alum-induced peritonitis is dependent on Syk and Jnk

Next we investigated whether Syk and Jnk were required for inflammasome activation *in vivo*. We analyzed the recruitment of inflammatory cells into the peritoneal cavity as an indicator of stimulant-induced inflammation after intraperitoneal injection of mice with MSU or alum. As shown before[12,29], both MSU and alum strongly induced the recruitment of cells, including Gr-1$^+$ F4/80$^-$ neutrophils and F4/80$^+$ monocytes and macrophages, in an ASC-dependent manner (**Supplementary Fig. 8a–f**). We then reconstituted irradiated wild-type mice with fetal liver cells to generate *Syk*$^{+/-}$ and *Syk*$^{-/-}$ chimeras or with bone marrow cells to generate wild-type, *Mapk8*$^{-/-}$ and *Mapk9*$^{-/-}$ chimeras. After challenge with MSU or alum, *Syk*$^{-/-}$ chimeras had fewer total cells, neutrophils, and monocytes-macrophages in the peritoneal cavity than did *Syk*$^{+/-}$ chimeras (**Fig. 8a,b,d–f**). After challenge with MSU, the number of peritoneal monocytes-macrophages tended to be lower in *Syk*$^{-/-}$ chimeras than in *Syk*$^{+/-}$ chimeras, but the difference between the groups was not statistically significant (**Fig. 8c**). The infiltration of inflammatory cells induced by MSU or alum was also lower in *Mapk8*$^{-/-}$ chimeras or in wild-type mice treated with

an inhibitor of Jnk than in wild-type chimeras or wild-type mice treated with vehicle only, respectively (**Fig. 8g–i** and **Supplementary Fig. 8a–f**). In contrast, the inflammasome-independent infiltration of inflammatory cells induced by chemokine CXCL1 (KC) was similar in $Syk^{+/-}$ and $Syk^{-/-}$ chimeras and in $Mapk8^{+/+}$ and $Mapk8^{-/-}$ chimeras (**Supplementary Fig. 8g–l**), and the inhibitor of Jnk did not reduce the infiltration of inflammatory cells induced by alum in ASC-deficient mice ($n = 3$; data not shown). These results suggested that signaling via Syk and Jnk was involved in the MSU- and alum-induced infiltration of inflammatory cells that was largely dependent on ASC.

DISCUSSION

The phosphorylation and dephosphorylation of proteins is important in controlling a wide range of biological processes, including innate and adaptive immunity and apoptosis[36,37]. The involvement of kinases such as PKC-δ, PKR, Syk, Lyn, PI(3)K, Erk and DAPK in inflammasome activation has been reported, yet the precise mechanism of their action has remained unclear. In particular, Syk has been demonstrated to contribute to the NLRP3 inflammasome in response to *C. albicans*, most probably due to its role in inducing ROS production[28,29,31,33]. NLRC4 is phosphorylated after stimulation with its ligands, and that phosphorylation is critical for inflammasome activation[27]. Here we showed that Syk and Jnk were involved in the activity of ASC-containing inflammasomes in macrophages via a mechanism that regulated the formation of ASC specks. We found that ASC was phosphorylated in a Syk- and Jnk-dependent manner at multiple sites, which most probably included Tyr144, which was essential for speck formation. The phosphorylation of ASC during inflammasome activation was required for activity of the NLRP3 and AIM2 inflammasomes. Thus, inflammasomes are regulated by protein kinases and perhaps by phosphatase(s) that target phosphorylated inflammasome components.

We identified Tyr144 of ASC as a critical residue for speck formation and a possible phosphorylation site. Consistent with that, phosphorylation of the corresponding residue in human ASC (Tyr146) has been disclosed in a patent application (Hornbeck, P. *et al.*, US patent application 2009/0325189 A1). The Y144F substitution in ASC completely abrogated the phosphorylation of ASC induced by overexpression of Syk or Jnk, which suggested that Tyr144 serves as a regulator of ASC phosphorylation mediated by those kinases. That tyrosine residue is evolutionary conserved. Tyr144 is located in the CARD, whereas published studies have shown that the pyrin domain of ASC is phosphorylated after stimulation with tumor-necrosis factor[34], which suggests the existence of other phosphorylation sites that might also contribute to inflammasome activity.

It remains unclear how signaling via Syk and Jnk regulates the formation of ASC specks. Transfection of HEK293 cells to express ASC together with Syk or Jnk or both did not result in the formation of ASC specks or the redistribution of ASC to the Triton X-100–insoluble fraction (data not shown), which suggested that phosphorylation of ASC itself was not sufficient to induce speck formation in the absence of stimuli of the inflammasome. Our results also suggested a crucial role for Syk and Jnk in the redistribution, rather than the dimerization or oligomerization, of ASC upon inflammasome activation. During the generation of ASC aggregates, monomeric ASC, which is diffusely distributed before stimulation, is rapidly translocated to a perinuclear speck in each cell. The formation of ASC specks is prevented by treatment with nocodazole, and ASC specks are located near the microtubule-organizing center[38], which suggests a possible role for microtubules in the migration of ASC during the step of speck formation. In our assays, most complexes of ASC and phosphorylated Jnk were located in or around the nucleus, and ASC remained diffusely distributed in the cytosol even after inflammasome activation in cells in which Syk or Jnk was inhibited genetically or pharmacologically. Thus, we speculate that Syk- and Jnk-mediated ASC phosphorylation may function as a molecular 'switch' that controls the migration of ASC along microtubules to the site of speck formation. Together, these results indicate that ASC speck formation is a consequence of multiple cellular events orchestrated by inflammasome receptors, Syk, Jnk and perhaps microtubules.

Although inflammasomes have pivotal roles in innate immunity to pathogens, excessive or dysregulated activation of inflammasomes, especially the NLRP3 inflammasome, has been linked to various autoinflammatory diseases and autoimmune diseases, including Muckle-Wells syndrome, inflammatory bowel diseases[39,40], vitiligo[41] and rheumatoid arthritis[12]. Inflammasomes have also been linked to obesity-induced insulin resistance[42], atherosclerosis[43] and gouty arthritis[44] and could represent potential targets for therapy. Therapies involving antibody to IL-1β appear to be effective in treating inflammatory disorders associated with deregulated inflammasome activity, and further understanding of the basic processes and mechanisms involved in inflammasome activation will provide additional strategies for controlling autoinflammatory conditions. Here we have shown that phosphorylation of the inflammasome component ASC regulates inflammasome activity. Thus, for example, compounds designated to specifically inhibit the phosphorylation of ASC may be promising drug candidates for the treatment of inflammasome-associated diseases, and antibodies specific to phosphorylated ASC may be useful for diagnostic and research purposes. Further investigation of the inflammasome will reveal the precise roles of kinases in inflammasome activation and may identify additional mechanisms for controlling inflammasome activity.

METHODS

Methods and any associated references are available in the online version of the paper.

Note: Any Supplementary Information and Source Data files are available in the online version of the paper.

ACKNOWLEDGMENTS

We thank J. Tschopp and the Institute for Arthritis Research for permission to use $Nlrp3^{-/-}$ mice; S.Taniguchi (Shinshu University) for $Pycard^{-/-}$ mice; K. Kuida (Millennium Pharmaceuticals) for $Casp1^{-/-}$ mice; T. Saito (RIKEN RCAI) for $Card9^{-/-}$ mice; K. Kawasaki (Doshisha Women's College) for *S.* Typhimurium 14028; H. Tsutsui (Hyogo Medical University) for $Nlrp3^{-/-}$, $Pycard^{-/-}$ and $Casp1^{-/-}$ mice; H. Hara (Saga University) for $Card9^{-/-}$ mice; M. Matsuura (Kyoto University) for *S.* Typhimurium 14028 and for U937 cells; H. Tanizaki (Kyoto University) for RAW264.7 cells; and K. Sada and Y. Tohyama for advice on Syk experiments. Supported by the Ministry of Education, Culture, Sports, Science and Technology of Japan, the Ministry of Health, Labour and Welfare of Japan, the Japan Society for the Promotion of Science and Medical Research Council UK (U117527252 for E.S. and V.T.).

AUTHOR CONTRIBUTIONS

H.H. initiated the study and designed and did the experiments with macrophages and peritonitis; K.T. designed and did the experiments with HEK293 cells; K.T., H.H. and M.M. wrote the manuscript; I.K. provided advice; R.F., E.H.-C. and Y.S. contributed to the experiments; J.M. provided the $Mapk8^{-/-}$ and $Mapk9^{-/-}$ mice; E.S. and V.T. provided the $Syk^{+/+}$, $Syk^{+/-}$ and $Syk^{-/-}$ fetal liver cells; and M.M. supervised the project.

COMPETING FINANCIAL INTERESTS

The authors declare no competing financial interests.

1. Martinon, F., Mayor, A. & Tschopp, J. The inflammasomes: guardians of the body. *Annu. Rev. Immunol.* **27**, 229–265 (2009).
2. Brodsky, I.E. & Monack, D. NLR-mediated control of inflammasome assembly in the host response against bacterial pathogens. *Semin. Immunol.* **21**, 199–207 (2009).
3. Davis, B.K., Wen, H. & Ting, J.P. The inflammasome NLRs in immunity, inflammation, and associated diseases. *Annu. Rev. Immunol.* **29**, 707–735 (2011).
4. Dinarello, C.A. Immunological and inflammatory functions of the interleukin-1 family. *Annu. Rev. Immunol.* **27**, 519–550 (2009).
5. Miao, E.A. *et al.* Innate immune detection of the type III secretion apparatus through the NLRC4 inflammasome. *Proc. Natl. Acad. Sci. USA* **107**, 3076–3080 (2010).
6. Franchi, L. *et al.* Cytosolic flagellin requires Ipaf for activation of caspase-1 and interleukin 1β in salmonella-infected macrophages. *Nat. Immunol.* **7**, 576–582 (2006).
7. Miao, E.A. *et al.* Cytoplasmic flagellin activates caspase-1 and secretion of interleukin 1beta via Ipaf. *Nat. Immunol.* **7**, 569–575 (2006).
8. Boyden, E.D. & Dietrich, W.F. Nalp1b controls mouse macrophage susceptibility to anthrax lethal toxin. *Nat. Genet.* **38**, 240–244 (2006).
9. Franchi, L., Munoz-Planillo, R., Reimer, T., Eigenbrod, T. & Nunez, G. Inflammasomes as microbial sensors. *Eur. J. Immunol.* **40**, 611–615 (2010).
10. Mariathasan, S. *et al.* Cryopyrin activates the inflammasome in response to toxins and ATP. *Nature* **440**, 228–232 (2006).
11. Kanneganti, T.D. *et al.* Critical role for Cryopyrin/Nalp3 in activation of caspase-1 in response to viral infection and double-stranded RNA. *J. Biol. Chem.* **281**, 36560–36568 (2006).
12. Martinon, F., Petrilli, V., Mayor, A., Tardivel, A. & Tschopp, J. Gout-associated uric acid crystals activate the NALP3 inflammasome. *Nature* **440**, 237–241 (2006).
13. Li, H., Nookala, S. & Re, F. Aluminum hydroxide adjuvants activate caspase-1 and induce IL-1beta and IL-18 release. *J. Immunol.* **178**, 5271–5276 (2007).
14. Rathinam, V.A. *et al.* The AIM2 inflammasome is essential for host defense against cytosolic bacteria and DNA viruses. *Nat. Immunol.* **11**, 395–402 (2010).
15. Fernandes-Alnemri, T. *et al.* The AIM2 inflammasome is critical for innate immunity to *Francisella tularensis*. *Nat. Immunol.* **11**, 385–393 (2010).
16. Tsuchiya, K. *et al.* Involvement of absent in melanoma 2 in inflammasome activation in macrophages infected with *Listeria monocytogenes*. *J. Immunol.* **185**, 1186–1195 (2010).
17. Kim, S. *et al. Listeria monocytogenes* is sensed by the NLRP3 and AIM2 inflammasome. *Eur. J. Immunol.* **40**, 1545–1551 (2010).
18. Fang, R. *et al.* Critical roles of ASC inflammasomes in caspase-1 activation and host innate resistance to *Streptococcus pneumoniae* infection. *J. Immunol.* **187**, 4890–4899 (2011).
19. Kerur, N. *et al.* IFI16 acts as a nuclear pathogen sensor to induce the inflammasome in response to Kaposi sarcoma-associated herpesvirus infection. *Cell Host Microbe* **9**, 363–375 (2011).
20. Masumoto, J. *et al.* ASC, a novel 22-kDa protein, aggregates during apoptosis of human promyelocytic leukemia HL-60 cells. *J. Biol. Chem.* **274**, 33835–33838 (1999).
21. Case, C.L., Shin, S. & Roy, C.R. Asc and Ipaf Inflammasomes direct distinct pathways for caspase-1 activation in response to *Legionella pneumophila*. *Infect. Immun.* **77**, 1981–1991 (2009).
22. Bryan, N.B., Dorfleutner, A., Rojanasakul, Y. & Stehlik, C. Activation of inflammasomes requires intracellular redistribution of the apoptotic speck-like protein containing a caspase recruitment domain. *J. Immunol.* **182**, 3173–3182 (2009).
23. Fernandes-Alnemri, T. *et al.* The pyroptosome: a supramolecular assembly of ASC dimers mediating inflammatory cell death via caspase-1 activation. *Cell Death Differ.* **14**, 1590–1604 (2007).
24. Guarda, G. *et al.* Type I interferon inhibits interleukin-1 production and inflammasome activation. *Immunity* **34**, 213–223 (2011).
25. Mayor, A., Martinon, F., De Smedt, T., Petrilli, V. & Tschopp, J. A crucial function of SGT1 and HSP90 in inflammasome activity links mammalian and plant innate immune responses. *Nat. Immunol.* **8**, 497–503 (2007).
26. Franchi, L. *et al.* Calcium-independent phospholipase A2β is dispensable in inflammasome activation and its inhibition by bromoenol lactone. *J. Innate Immun.* **1**, 607–617 (2009).
27. Qu, Y. *et al.* Phosphorylation of NLRC4 is critical for inflammasome activation. *Nature* **490**, 539–542 (2012).
28. Gross, O. *et al.* Syk kinase signalling couples to the Nlrp3 inflammasome for anti-fungal host defence. *Nature* **459**, 433–436 (2009).
29. Shio, M.T. *et al.* Malarial hemozoin activates the NLRP3 inflammasome through Lyn and Syk kinases. *PLoS Pathog.* **5**, e1000559 (2009).
30. Chuang, Y.T. *et al.* Tumor suppressor death-associated protein kinase is required for full IL-1β production. *Blood* **117**, 960–970 (2011).
31. Kankkunen, P. *et al.* (1,3)-beta-glucans activate both dectin-1 and NLRP3 inflammasome in human macrophages. *J. Immunol.* **184**, 6335–6342 (2010).
32. Lu, B. *et al.* Novel role of PKR in inflammasome activation and HMGB1 release. *Nature* **488**, 670–674 (2012).
33. Wong, K.W. & Jacobs, W.R. Jr. Critical role for NLRP3 in necrotic death triggered by *Mycobacterium tuberculosis*. *Cell Microbiol.* **13**, 1371–1384 (2011).
34. Stehlik, C. *et al.* The PAAD/PYRIN-only protein POP1/ASC2 is a modulator of ASC-mediated nuclear-factor-κB and pro-caspase-1 regulation. *Biochem. J.* **373**, 101–113 (2003).
35. Kosako, H. *et al.* Phosphoproteomics reveals new ERK MAP kinase targets and links ERK to nucleoporin-mediated nuclear transport. *Nat. Struct. Mol. Biol.* **16**, 1026–1035 (2009).
36. Kurokawa, M. & Kornbluth, S. Caspases and kinases in a death grip. *Cell* **138**, 838–854 (2009).
37. Sumbayev, V.V. & Yasinska, I.M. Role of MAP kinase-dependent apoptotic pathway in innate immune responses and viral infection. *Scand. J. Immunol.* **63**, 391–400 (2006).
38. Balci-Peynircioglu, B. *et al.* Expression of ASC in renal tissues of familial mediterranean fever patients with amyloidosis: postulating a role for ASC in AA type amyloid deposition. *Exp. Biol. Med. (Maywood)* **233**, 1324–1333 (2008).
39. Villani, A.C. *et al.* Common variants in the NLRP3 region contribute to Crohn's disease susceptibility. *Nat. Genet.* **41**, 71–76 (2009).
40. Zaki, M.H. *et al.* The NLRP3 inflammasome protects against loss of epithelial integrity and mortality during experimental colitis. *Immunity* **32**, 379–391 (2010).
41. Jin, Y. *et al.* NALP1 in vitiligo-associated multiple autoimmune disease. *N. Engl. J. Med.* **356**, 1216–1225 (2007).
42. Vandanmagsar, B. *et al.* The NLRP3 inflammasome instigates obesity-induced inflammation and insulin resistance. *Nat. Med.* **17**, 179–188 (2011).
43. Duewell, P. *et al.* NLRP3 inflammasomes are required for atherogenesis and activated by cholesterol crystals. *Nature* **464**, 1357–1361 (2010).
44. Pope, R.M. & Tschopp, J. The role of interleukin-1 and the inflammasome in gout: implications for therapy. *Arthritis Rheum.* **56**, 3183–3188 (2007).

ONLINE METHODS

Mice. Female wild-type, *Casp1*$^{-/-}$, *Pycard*$^{-/-}$, *Nlrp3*$^{-/-}$, *Card9*$^{-/-}$, *Mapk8*$^{-/-}$ and *Mapk9*$^{-/-}$C57BL/6J mice were maintained in specific pathogen–free conditions and were used at 6–9 weeks of age[12,16,45,46]. C57BL/6J mice heterozygous for the *Syk*^{tm1Tyb} allele[47] were intercrossed to generate embryos at embryonic day 16.5 that were wild-type for *Syk* (*Syk*$^{+/+}$) or heterozygous or homozygous for the *Syk*^{tm1Tyb} allele (*Syk*$^{+/-}$ or *Syk*$^{-/-}$). Fetal liver cells from those embryos were used to reconstitute C57BL/6J mice that had been irradiated with a total dose of 10 Gy from a ^{137}Cs source. Bone marrow cells from wild-type, *Mapk8*$^{-/-}$ or *Mapk9*$^{-/-}$ mice were also used to reconstitute irradiated C57BL/6J mice. Mice were used 6–7 weeks after reconstitution. All the experimental procedures performed on mice were approved by the Animal Ethics and Research Committee of Kyoto University Graduate School of Medicine.

Cells. Peritoneal macrophages, bone marrow–derived macrophages and bone marrow–derived dendritic cells were prepared as reported[48,49]. Those cells suspended in culture medium consisted of RPMI-1640 medium supplemented with 10% FCS and 10 μg/ml gentamicin were incubated on culture plates overnight at 37 °C, then were used for this study. U937 cells (provided by M. Matsuura) were cultured for 3 d in culture medium supplemented with 10 ng/ml of 12-*O*-tetradecanoylphorbol 13-acetate, 100 U/ml of penicillin and 100 μg/ml of streptomycin. The order of treatment and positions of wells in multiwell devices were determined randomly.

Reagents. LPS and flagellin were from Invivogen; alum was from Pierce; nigericin and poly(dA:dT) were from Sigma-Aldrich; MSU was from Nacalai Tesque; R406 was from Selleckchem; other kinase inhibitors were from Merck Biosciences; and BHA (butylated hydroxyanisole) was from Wako. Polyclonal antibody to ASC (AL177) and mouse monoclonal antibody (mAb) to NLRP3 (Cryo-2) were from Alexis; mAb to Jnk (56G8), mAb to phosphorylated Jnk (81E11) and mouse mAb to phosphorylated Jnk (G9) were from Cell Signaling Technology; mAb to phosphorylated Tyr (PY20), antibody to caspase-1 p10 (M-20) and antibody to Syk (anti-Syk) (N-19) were from Santa Cruz; anti-Flag (600-401-383) was from Rockland Immunochemicals; biotin-conjugated anti-IL-1β (BAF401) was from R&D Systems; and mAb to IL-18 (39-3F) was from MBL. The enzyme-linked immunosorbent assay kit for mouse IL-1β was from eBioscience. For the 'titration' of human or mouse IL-18, a pair of biotin-labeled (93-10C) and unlabeled (74) monoclonal antibodies to IL-18 was used (both from MBL).

Plasmids. The plasmid pmax-GFP was from Lonza. The pFLAG expression vectors for ASC, pro-caspase-1, and pro-IL-1β were constructed before[16]. The expression vectors for NLRP3 (R258W), Syk, Jnk1 (isoform β2) and Jnk2 (isoform β2) were constructed with primer sets (**Supplementary Table 3**) and the pFLAG-CMV2 vector (Sigma-Aldrich). After that construction, the mutation in the gene encoding NLRP3 or ASC was introduced into each expression vector by site-directed mutagenesis. Similarly, pFLAG–pro-caspase-1 and pFLAG–pro-IL-1β in which the Flag tag was removed were generated.

Stimulation with inflammasome activators. Cells were plated at a density of 5×10^5 cells per well in 24-well microplates. Culture medium was replaced with Opti-MEM (Invitrogen) before stimulation or infection. Macrophages were primed for 4 h with 50 ng/ml LPS and stimulated with nigericin (5 μM) or alum (500 μg/ml). For delivery into the cytosol of macrophages, flagellin (15 ng) was encapsulated into Sendai virus envelope with GenomONE-Neo (Ishihara Sangyo). Poly(dA:dT) (2.6 μg/ml) was introduced into unprimed macrophages through the use of Lipofectamine LTX (Invitrogen). Cells were infected with *L. monocytogenes* EGD[48] (multiplicity of infection, 1) or *S.* Typhimurium 14028 (multiplicity of infection, 10), and gentamicin was added to the cultures 30 min after infection. Cells infected with *M. tuberculosis* H37Rv (multiplicity of infection, 5) were washed 3 h after infection and were further cultivated in Opti-MEM containing gentamicin. Kinase inhibitors or dimethyl sulfoxide were added to cell cultures 1 h before stimulation or infection for inflammasome activation.

Immunoblot analysis. Cells were lysed with SDS sample buffer. Supernatants were concentrated with trichloroacetate. For the generation of Triton X-100–soluble and Triton X-100–insoluble fractions, cells were lysed with 50 mM Tris-HCl (pH 7.6) containing 0.5% Triton X-100, EDTA-free protease inhibitor 'cocktail' and phosphatase inhibitor 'cocktail' (Nacalai tesque). The lysates were centrifuged at 6,000*g* at 4 °C for 15 min, and the pellets and supernatants were used as the Triton-insoluble and Triton-soluble fractions, respectively. For the detection of phosphorylated Syk, total Syk was immunoprecipitated with anti-Syk (N-19; Santa Cruz) and protein G Sepharose (GE Healthcare).

Crosslinkage of ASC dimers or oligomers. The Triton-insoluble pellets were washed twice with Tris-buffered saline and then resuspended in 500 μl Tris-buffered saline. The resuspended pellets were crosslinked for 45 min at 37 °C with 2 mM disuccinimidyl suberate (Pierce) and then centrifuged for 15 min at 6,000*g*. The pellets were dissolved in SDS sample buffer.

Enrichment of phosphorylated proteins. Phosphorylated proteins were enriched from cell lysates with a Pro-Q Diamond Phosphoprotein Enrichment Kit according to the manufacturer's instructions (Invitrogen). Cells were lysed in lysis buffer supplemented with inhibitors of endonuclease and proteinase, then ASC aggregates were solubilized with 8 M urea. After centrifugation for 10 min at 10,000*g*, the supernatants were applied to the Pro-Q diamond column (1 mg protein per column). The column was washed and eluted with elution buffer (50 mM Tris, 2% SDS, 10 mM EDTA and 5% 2-mercaptoethanol, pH 8). The flow-through and elution fractions were concentrated with trichloroacetate. ASC or phosphorylated tyrosine in each fraction was detected by immunoblot analysis.

Phos-tag-based MSA. The Triton X-100–insoluble and Triton X-100–soluble fractions from macrophages (prepared as described above) were analyzed by Phos-tag MSA. HEK293 cells were lysed with 50 mM Tris-HCl (pH 7.6) containing 1% SDS, then lysates were precipitated with isopropanol and acetone. Proteins in the lysates were precipitated with acetone, incubated overnight at 37 °C in phosphatase reaction mixture containing 250 U/ml of antarctic phosphatase (New England BioLabs), reprecipitated with acetone and dissolved in SDS sample buffer. Those samples were separated by electrophoresis through 12% polyacrylamide gels with or without 50 μM $MnCl_2$ and 25 μM Phos-tag ligand (NARD Institute).

RNA-mediated interference. Cells were transfected with 30 nM small interfering RNA through the use of the siPORT Amine Transfection Agent (Ambion) as reported[16]. After 48 h of cultivation, the cells were washed and used in experiments. The sense small interfering RNA sequences were as follows: *Syk* (A), ACUUGUAGUAGUUGAUGCAUUCGGG; *Syk* (B), AUUCCGAUCAUGCG CACAAUGUAGG; *Mapk8* (A), AAUAUAGUCCCUUCCUGGAAAGAGG; *Mapk8* (B), AAUUCCAGCAGAGUGAAGGUGCUUG; *Mapk9* (A), UAAA GUUGGUACAGGCUGUUCGCGC; and *Mapk9* (B), UUCAAUCGCAUGC UCUCUUUCUUCC. Stealth RNAi negative control medium GC duplex #3 was from Invitrogen.

Immunofluorescence staining. Cells seeded in eight-well chamber plates at a density of 2.5×10^5 cells per well were washed twice, fixed in 4% paraformaldehyde and permeabilized with 0.25% Triton X-100. The cells were incubated with anti-ASC (AL177; Alexis) and then with Alexa 488-labeled or Alexa 594-labeled antibody to rabbit IgG (A11034 or A11012; Invitrogen). Nuclei were stained with DAPI (4,6-diamidino-2-phenylindole; Dojindo).

***In situ* PLA.** Fixed and permeabilized cells were incubated overnight at 4 °C with the following pairs of primary antibodies: rabbit anti-ASC (AL177; Alexis) together with mouse mAb to phosphorylated Jnk (G9; Cell Signaling) or mouse mAb to NLRP3 (Cryo-2; Alexis). The cells were washed and allowed to react to a pair of proximity probes (Olink Bioscience). The rest of the *in situ* PLA protocol was performed according to the manufacturer's instructions. The cells were examined by fluorescence microscopy (Olympus), and the Duolink Image Tool (Olink Bioscience) was used for quantitative analysis.

Reconstruction of the inflammasome system in HEK293 cells. HEK293 cells (CRL-1573; American Type Culture Collection) were maintained in DMEM supplemented with 10% FCS, 6 mM L-glutamine, 1 mM sodium pyruvate and

doi:10.1038/ni.2749

5 μg/ml gentamicin as described[16]. For experiments, HEK293 cells were plated in 24-well microplates at a density of 2×10^5 cells per well and incubated overnight. The cells were transfected with plasmids through the use of Transfectin according to the manufacturer's instructions (Bio-Rad). The total amount of DNA was adjusted to a concentration of 1 μg per well with pFLAG-CMV2 empty vector. The cells were washed with culture medium 36 h after transfection and were further incubated for 12 h.

Reconstruction in macrophages. RAW264.7 cells (provided by H. Tanizaki) or primary *Pycard*$^{-/-}$ peritoneal macrophages were transfected with 1,000 ng of pFLAG-ASC or the ASC mutant vectors together with pFLAG-NLRP3 (R258W) (250 ng) through the use of the Neon Transfection System according to the manufacturer's instructions (Invitrogen). Electroporation parameters were as follows: pulse voltage, 1,680 V; pulse width, 20 ms; pulse number, 1; cell number, 1×10^6. The cells were incubated for 9 h.

Peritonitis. Mice were challenged intraperitoneally with MSU (1 mg) or alum (0.4 mg). At 2 h before and 30 min after challenge with the irritants, wild-type mice were treated intraperitoneally with dimethyl sulfoxide or the Jnk inhibitor SP600125 (25 mg per kg body weight). The mice were killed 6 h after injection of the stimuli, and peritoneal cavities were lavaged with 5 ml PBS. Mice were given intraperitoneal injection of mouse CXCL1 (0.8 μg; BioLegend) or PBS, and peritoneal cells were collected 1.5 h after stimulation. Peritoneal cells were counted with a Countess (Invitrogen) and then were allowed to react to mAb to mouse CD16 (93; BioLegend). The cells were subsequently stained with fluorescein isothiocyanate–labeled mAb to Gr-1 (RB6-8C5; BioLegend) and phycoerythrin-labeled mAb to F4/80 (BM8; BioLegend) and were analyzed on a FACSCalibur (Becton Dickinson). Mice were prepared by H.H. and were randomly assigned to experimental groups. Another investigator (R.F.), who did the injections and flow cytometry, was 'blinded' to the identity of the groups.

Statistical analysis. The sample size of *in vivo* and *in vitro* studies was chosen to be as small as possible but to allow the evaluation of distribution normality. For two-group comparisons by Gaussian distribution, a two-tailed unpaired *t*-test with Welch's correction was used when the variances of the groups were judged to be equal by the *F* test. For two-group comparisons with non-Gaussian distribution, a Mann-Whitney test was used. Multigroup comparisons with Gaussian distribution, one-way ANOVA with Bonferroni's multiple-comparison test or Tukey-Kramer's multiple-comparison test (for samples of unequal size) was used after the confirmation of homogeneity of variance among the groups by Bartlett's test. For multigroup comparisons with non-Gaussian distribution, a Kruskal-Wallis test with Dunn's test was used. *P* values of 0.05 or less were the threshold for statistical significance.

45. Hara, H. *et al.* The adaptor protein CARD9 is essential for the activation of myeloid cells through ITAM-associated and Toll-like receptors. *Nat. Immunol.* **8**, 619–629 (2007).
46. Cao, Y. *et al.* Enhanced T cell-independent antibody responses in c-Jun N-terminal kinase 2 (JNK2)-deficient B cells following stimulation with CpG-1826 and anti-IgM. *Immunol. Lett.* **132**, 38–44 (2010).
47. Turner, M. *et al.* Perinatal lethality and blocked B-cell development in mice lacking the tyrosine kinase Syk. *Nature* **378**, 298–302 (1995).
48. Hara, H. *et al.* Dependency of caspase-1 activation induced in macrophages by *Listeria monocytogenes* on cytolysin, listeriolysin O, after evasion from phagosome into the cytoplasm. *J. Immunol.* **180**, 7859–7868 (2008).
49. Lutz, M.B. *et al.* An advanced culture method for generating large quantities of highly pure dendritic cells from mouse bone marrow. *J. Immunol. Methods* **223**, 77–92 (1999).

Infection, Genetics and Evolution 16 (2013) 151–156

Contents lists available at SciVerse ScienceDirect

Infection, Genetics and Evolution

journal homepage: www.elsevier.com/locate/meegid

Two genetically-related multidrug-resistant *Mycobacterium tuberculosis* strains induce divergent outcomes of infection in two human macrophage models

Noemí Yokobori [a,*], Beatriz López [b], Laura Geffner [a], Carmen Sabio y García [a], Pablo Schierloh [a], Lucía Barrera [b], Silvia de la Barrera [a], Shunsuke Sakai [c], Ikuo Kawamura [c], Masao Mitsuyama [c], Viviana Ritacco [b], María del Carmen Sasiain [a]

[a] Instituto de Medicina Experimental (IMEX) – CONICET, Academia Nacional de Medicina, Pacheco de Melo 3081, (C1425ASU) Buenos Aires, Argentina
[b] Instituto Nacional de Enfermedades Infecciosas ANLIS "Carlos G. Malbrán", Vélez Sarsfield 563, (C1282AFR) Buenos Aires, Argentina
[c] Graduate School of Medicine, Kyoto University, Yoshidakonoe-cho, Sakyo-ku, (606-8501) Kyoto, Japan

ARTICLE INFO

Article history:
Received 20 September 2012
Received in revised form 4 January 2013
Accepted 9 January 2013
Available online 24 January 2013

Keywords:
Multidrug resistance
Mycobacterium tuberculosis
Monocyte derived macrophages
U937
Virulence
Cytokines

ABSTRACT

Mycobacterium tuberculosis has a considerable degree of genetic variability resulting in different epidemiology and disease outcomes. We evaluated the pathogen-host cell interaction of two genetically closely-related multidrug-resistant *M. tuberculosis* strains of the Haarlem family, namely the strain M, responsible for an extensive multidrug-resistant tuberculosis outbreak, and its kin strain 410 which caused a single case in two decades. Intracellular growth and cytokine responses were evaluated in human monocyte-derived macrophages and dU937 macrophage-like cells. In monocyte-derived macrophages, strain M grew more slowly and induced lower levels of TNF-α and IL-10 than 410, contrasting with previous studies with other strains, where a direct correlation was observed between increased intracellular growth and epidemiological success. On the other hand, in dU937 cells, no difference in growth was observed between both strains, and strain M induced significantly higher TNF-α levels than strain 410. We found that both cell models differed critically in the expression of receptors for *M. tuberculosis* entry, which might explain the different infection outcomes. Our results in monocyte-derived macrophages suggest that strain M relies on a modest replication rate and cytokine induction, keeping a state of quiescence and remaining rather unnoticed by the host. Collectively, our results underscore the impact of *M. tuberculosis* intra-species variations on the outcome of host cell infection and show that results can differ depending on the *in vitro* infection model.

1. Introduction

Tuberculosis (TB) remains a major cause of suffering and death worldwide. The HIV/AIDS pandemic, the decline of public health systems and the emergence of multidrug-resistant (MDR) *Mycobacterium tuberculosis* strains have contributed to the global upsurge of TB observed towards the turn of the millennium. This unexpected re-emergence of the disease, which until then had been deemed to be close to elimination (Paolo and Nosanchuk, 2004), prompted a strengthening of control policies and also boosted research on TB.

In the early '90s, a large AIDS-related MDR-TB outbreak occurred in hospitals located in Buenos Aires, Argentina (Ritacco et al., 1997), which thereafter disseminated to immunocompetent individuals (Palmero et al., 2003). Epidemiological, bacteriological and genotyping data have allowed the identification of the so-called strain M, which belongs to the Haarlem family (subfamily H2) and is responsible for the largest reported MDR-TB cluster in Latin America (Ritacco et al., 2012a). This highly successful genotype has been able to prevail over other MDR *M. tuberculosis* strains and to persist in the community. It still accounts for one in every 3.5 new MDR-TB cases in Argentina (Ritacco et al., 2012b). Another MDR strain closely related to strain M, the strain 410, was first identified at the early epidemic as having a single band difference in the IS*6110* RFLP pattern (Geffner et al., 2009, Supplementary Fig. 1). Strain 410 caused one MDR-TB case which has remained unique, suggesting that it has an impaired ability to cause active disease in new hosts.

Molecular epidemiology studies revealed that *M. tuberculosis*, previously regarded as a highly conserved species, has a considerable degree of genetic variability, and mounting evidence suggests that intrinsic properties of certain *M. tuberculosis* genotypes might

Abbreviations: MDM, monocyte-derived macrophages; MDR, multidrug-resistant; TB, tuberculosis; RFLP, restriction fragment length polymorphism; dU937, PMA-differentiated U937 cells; CFU, colony forming units; AFB, acid-fast bacilli; MR, mannose receptor; MOI, multiplicity of infection.

* Corresponding author. Tel.: +54 11 4805 5695x240; fax: +54 11 4805 0712.
E-mail address: kaoru.noemi@gmail.com (N. Yokobori).

1567-1348/$ - see front matter © 2013 Elsevier B.V. All rights reserved.
http://dx.doi.org/10.1016/j.meegid.2013.01.007